Elsevier has created a Monkeypox Information Center in response to the declared public health emergency of international concern, with free information in English on the monkeypox virus. The Monkeypox Information Center is hosted on Elsevier Connect, the company's public news and information website.

Elsevier hereby grants permission to make all its monkeypox related research that is available on the Monkeypox Information Center - including this research content - immediately available in publicly funded repositories, with rights for unrestricted research re-use and analyses in any form or by any means with acknowledgement of the original source. These permissions are granted for free by Elsevier for as long as the Monkeypox Information Center remains active.

Biosensors and Bioelectronics 220 (2023) 114847

Contents lists available at ScienceDirect

Biosensors and Bioelectronics

journal homepage: www.elsevier.com/locate/bios

Towards hospital-on-chip supported by 2D MXenes-based 5th generation intelligent biosensors

Vishal Chaudhary [a,b,1,**], Virat Khanna [c,1], Hafiz Taimoor Ahmed Awan [d], Kamaljit Singh [c], Mohammad Khalid [d,e], Yogendra Kumar Mishra [f], Shekhar Bhansali [g], Chen-Zhong Li [h,i,***], Ajeet Kaushik [j,k,*]

[a] Research Cell & Department of Physics, Bhagini Nivedita College, University of Delhi, Delhi, 110043, India
[b] SUMAN Laboratory (SUstainable Materials & Advanced Nanotechnology Lab), New Delhi 110072, India
[c] Department of Mechanical Engineering, MAIT, Maharaja Agrasen University, HP, 174103, India
[d] Graphene & Advanced 2D Materials Research Group (GAMRG), School of Engineering and Technology, Sunway University, No. 5, Jalan University, Bandar Sunway, 47500, Petaling Jaya, Selangor, Malaysia
[e] Sunway Materials Smart Science & Engineering (SMS2E) Research Cluster, Sunway University, No. 5, Jalan Universiti, Bandar Sunway, 47500, Petaling Jaya, Selangor, Malaysia
[f] Mads Clausen Institute, NanoSYD, University of Southern Denmark, Alison 2, Sønderborg, 6400, Denmark
[g] Department of Electrical and Computing Engineering, Florida International University, Miami, FL, 33174, USA
[h] Center for Cellular and Molecular Diagnostics, Tulane University School of Medicine, 1430 Tulane Ave., New Orleans, LA, 70112, USA
[i] Department of Biochemistry and Molecular Biology, Tulane University School of Medicine, 1430 Tulane Ave., New Orleans, LA, 70112, USA
[j] NanoBioTech Laboratory, Department of Environmental Engineering, Florida Polytechnic University, Lakeland, FL, 33805, USA
[k] School of Engineering, University of Petroleum and Energy Studies (UPES), Dehradun, Uttarakhand, India

ARTICLE INFO

Keywords:
MXenes
5th generation biosensor
Hospital-on-chip
Personalized diagnostics
Lab-on-chip

ABSTRACT

Existing public health emergencies due to fatal/infectious diseases such as coronavirus disease (COVID-19) and monkeypox have raised the paradigm of 5th generation portable intelligent and multifunctional biosensors embedded on a single chip. The state-of-the-art 5th generation biosensors are concerned with integrating advanced functional materials with controllable physicochemical attributes and optimal machine processability. In this direction, 2D metal carbides and nitrides (MXenes), owing to their enhanced effective surface area, tunable physicochemical properties, and rich surface functionalities, have shown promising performances in biosensing flatlands. Moreover, their hybridization with diversified nanomaterials caters to their associated challenges for the commercialization of stability due to restacking and oxidation. MXenes and its hybrid biosensors have demonstrated intelligent and lab-on-chip prospects for determining diverse biomarkers/pathogens related to fatal and infectious diseases. Recently, on-site detection has been clubbed with solution-on-chip MXenes by interfacing biosensors with modern-age technologies, including 5G communication, internet-of-medical-things (IoMT), artificial intelligence (AI), and data clouding to progress toward hospital-on-chip (HOC) modules. This review comprehensively summarizes the state-of-the-art MXene fabrication, advancements in physicochemical properties to architect biosensors, and the progress of MXene-based lab-on-chip biosensors toward HOC solutions. Besides, it discusses sustainable aspects, practical challenges and alternative solutions associated with these modules to develop personalized and remote healthcare solutions for every individual in the world.

* Corresponding author. NanoBioTech Laboratory, Health System Engineering, Department of Environmental Engineering, Florida Polytechnic University, Lakeland, FL 33805, USA.
** Corresponding author. Research Cell & Department of Physics, Bhagini Nivedita College, University of Delhi, Delhi, 110043, India.
*** Corresponding author. Center for Cellular and Molecular Diagnostics, Tulane University School of Medicine, 1430 Tulane Ave., New Orleans, LA, 70112, USA.
E-mail addresses: Chaudhary00vishal@gmail.com (V. Chaudhary), chenzhongbiosensor@gmail.com (C.-Z. Li), akaushik@floridapoly.edu (A. Kaushik).
[1] Equal First Contributor.

https://doi.org/10.1016/j.bios.2022.114847
Received 2 August 2022; Received in revised form 19 September 2022; Accepted 20 October 2022
Available online 27 October 2022

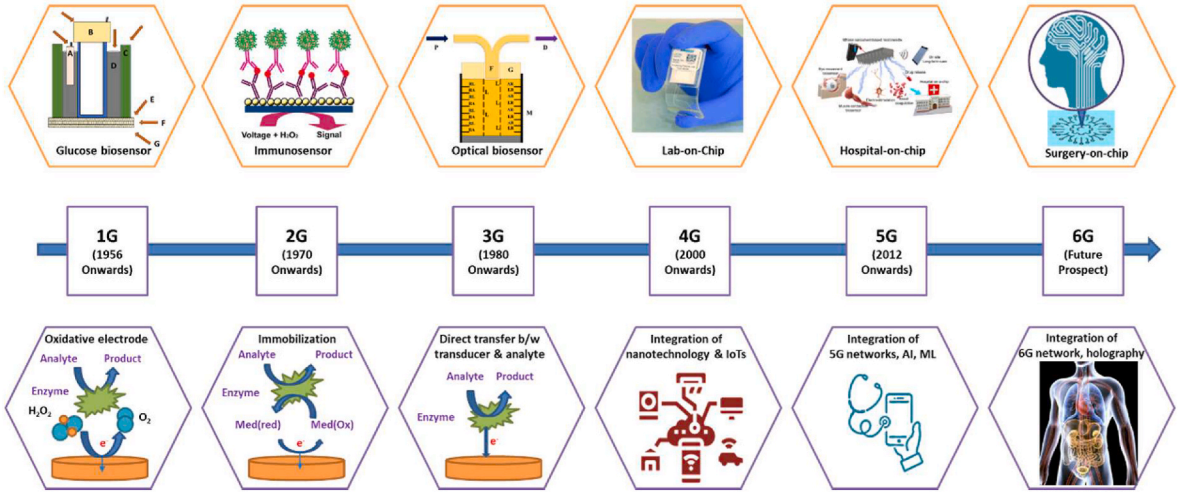

Fig. 1. Timeline for evolution of biosensors from 1st generation to 5th generation with prospects of 6th generation modules; subparts adapted from: Glucose biosensor ((Clark and Lyons, 2006)), Immunosensor ((Mani et al., 2009)), Optical biosensor ((Seitz, 1984)), Lab-on-chip ((Kukhtin et al., 2019)), Hospital-on-chip ((Yang et al., 2021)).

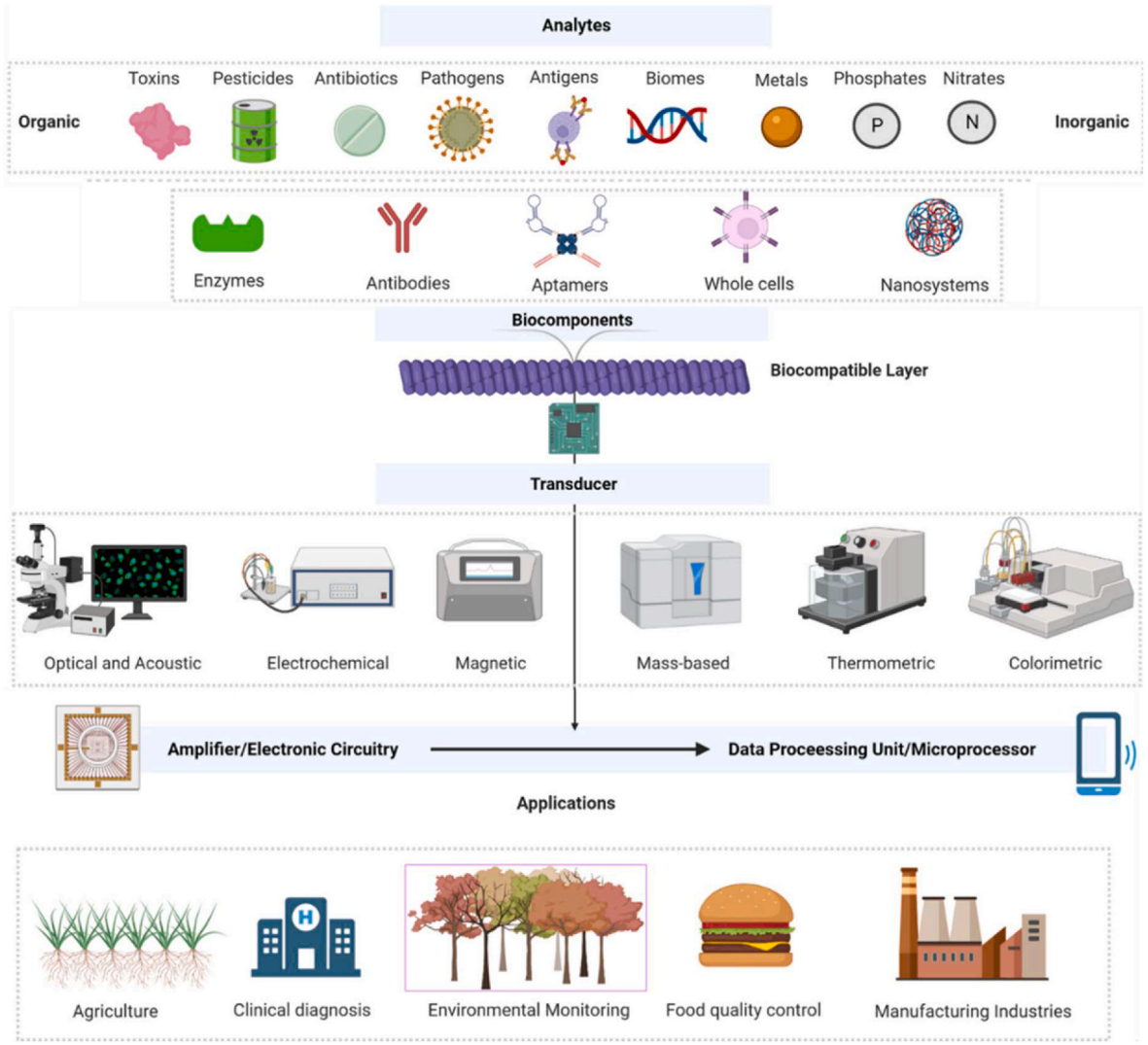

Fig. 2. Schematic illustration representing the fundamental biosensor components and detecting module for diversified applications. Created using BioRender.com.

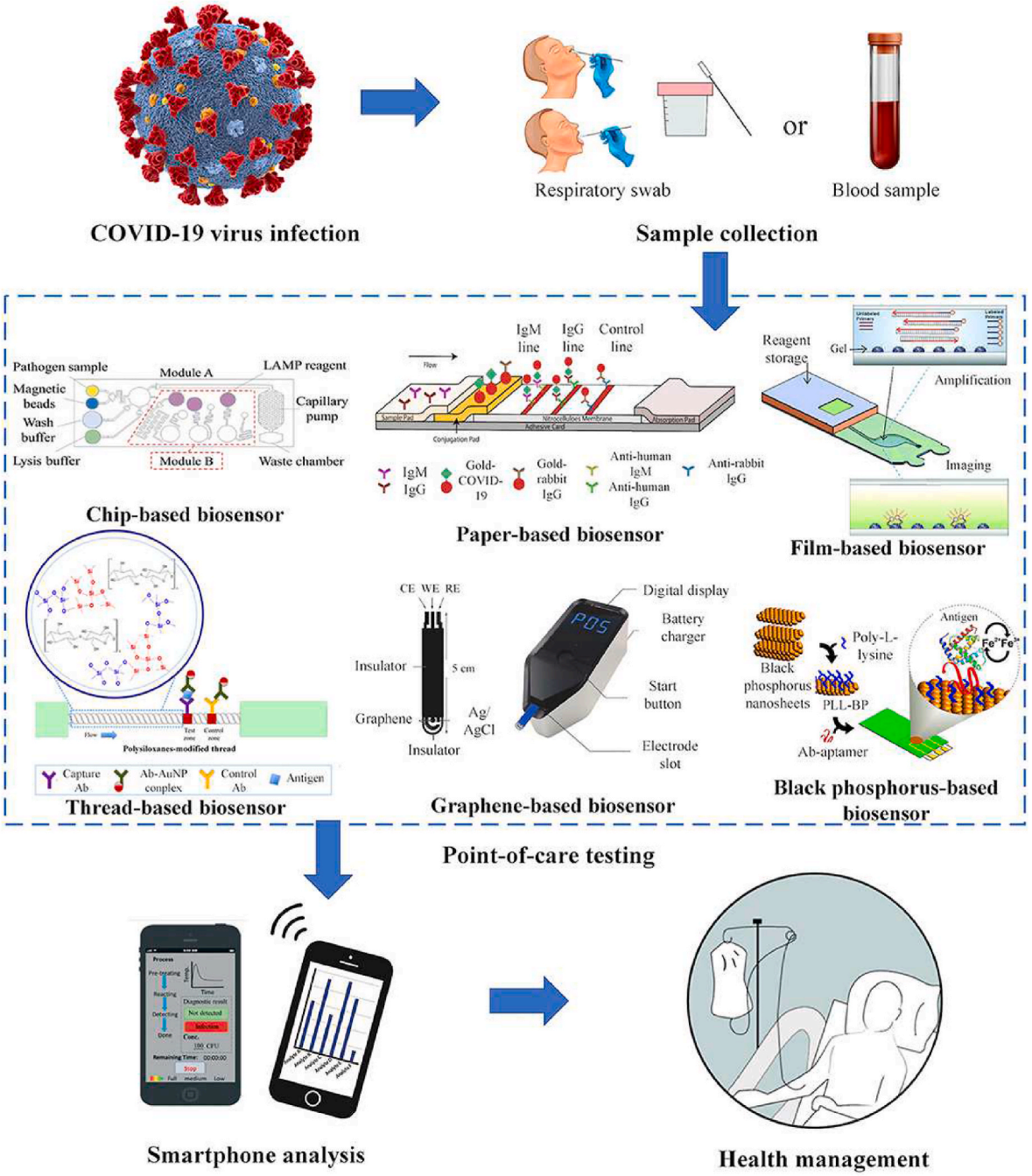

Fig. 3. Different types of point-of-care LOC biosensors for detecting SARS-CoV-2 (Choi, 2020).

1. Emergence of 5th generation biosensing strategies

The latent of biosensors have been extensively explored as plausible alternatives to the time-consuming, costly, complex and massive conventional diagnostics utilized in health care sectors (Patel et al., 2016; Solanki et al., 2011; Verma and Bhardwaj, 2015). Biosensors possess diversified applications, including biomedical sectors, pharmaceutical industries, hospitals and clinical treatment, healthcare centers, and personalized healthcare equipment. These biosensors are ideally installed for multiple disease recognition, human health organization, prevention, patient health observation and rehabilitation. Besides, biosensing devices are also implemented for the virus microorganisms, micro-organisms, pathogens and bacterial exposure (Dwivedi et al., 2021; Lei et al., 2019; Novoselov et al., 2004; Patel et al., 2016; Solanki et al., 2011).

Over time, applications and with temporal necessities, biosensors have evolved from 1st generation biosensors to 5th generation biosensors with the integration of developing technologies (Fig. 1).

The fundamentals of biosensor development commenced with *in vitro* investigations performed to mimic the sensory capabilities of living organisms. Clark and Lyons in 1962(Clark and Lyons, 2006) reported the first biosensor to detect glucose based on oxidation reaction utilizing an enzyme electrode. This pioneering work was followed by several studies based on potentiometric detection of biomolecules like urea, ushering in the era of 1st generation biosensors. However, in order to improve detection efficacy, simplify operation, and advance diagnostic quality, the 2nd generation of biosensors was introduced with a modified monitoring technique (Ansari and Malhotra, 2022; Kim et al., 2019; Xin

et al., 2020). It included co-immobilization of auxiliary enzymes or/and co-reactants through analyte (like biomolecules) converting enzymes. These modifications defined the basic structure and components of a biosensor, including sensing surface, transducers and analytical circuitry (Scheller et al., 1991). For instance, the transducer attached to biosensing layers was modified with enzymes/chemicals to achieve maximal and quality detection output like ELISA (enzyme-linked immunosorbent assay) based biosensors (Scheller et al., 1991).

Following these developments, the International Union of Pure and Applied Chemistry (IUPAC) recognized the term "biosensor" in 1996 and defined it as "A device that uses specific biochemical reactions mediated by isolated enzymes, immune systems, tissues, organelles or whole cells to detect chemical compounds usually by electrical, thermal or optical signals." However, the immobilization of sensing electrode with mediating-enzyme raised leaching susceptibility and the indirect interaction amongst the analyte and transducer affected the biosensor efficacies. Thus, the challenges in reproducibility, selectivity and stability raised the development of 3rd generation biosensors. The fundamentals of 3rd generation biosensors was based on direct communication between transducer and analyte, which enhances their monitory output quality, stability and efficacies (Gorton et al., 1999; Zhang and Li, 2004). It further recognized the different types of biosensors classified based on transducing mechanisms into electrochemical, optical and thermal biosensors (Kim et al., 2019; Zhang and Li, 2004)s. The first three-generation biosensors were concerned with modifications in detection fundamentals and mechanisms to achieve high performances. However, the 4th generation onwards of biosensors is the integration of developing technologies to diversify their utilization, enhance their efficacies, and move towards everything-on-single-chip modules (Kim et al., 2019; Solanki et al., 2011).

These biosensor technologies are based on nanomaterials as biological sensing components integrated with internet-of-things (IoTs) and rapid data processing modules within a transducer arrangement (Kaushik et al., 2018; Patel et al., 2016; Verma and Bhardwaj, 2015). It has three fundamental components, including the sensor to detect the stimulus/biomolecules, a transducer to adapt the stimulus to generate output signals, and processing of the sensory signal to build the output source in representable form, as illustrated in Fig. 2.

With the requirements of portable, personalized, and compact healthcare necessities, 4th generation biosensors are the integration of flexible, wearable, and nano-micro- electronics/technology with IoTs. It is concerned with the miniaturization of biosensor architect for point-of-care detection, such as lab-on-chip (LOC) modules. This has shifted the paradigm of conventional biosensors toward everything on a single chip, termed LOC module biosensors (S.-J. Liu et al., 2022; Y. Wang et al., 2022). The LOC biosensors are miniaturized devices designed with all the excellent functionalities and parameters incorporated into one platform, from the fabrication of samples to signal delivery processing to internet-of-nano-things (IoNTs)(Chaudhary et al., 2022; Cherusseri et al., 2022; Sonu and Chaudhary, 2022).

An ideal LOC device contains maximum robustness and strong-wired intelligence to employ the personal skilled free and transport the outcomes directly to the chief monitoring station (Besher et al., 2021; Xin et al., 2020). This device also supports distinguishing the biomolecule parameters, such as RNA and DNA variations. The significant development utilized to produce lab-on-a-chip is molecular biotechnology and microfluidics systems. Most importantly, these sorts of devices are prepared through extensive microchannels enclosed with antigens, oligonucleotides, and antibodies, which permit loads of biochemical reactions produced from the lone blood drop. Usually, glass, silicone, PDMS, thermoplastic polymers and multiple paper-related schemes are applied to develop LOC biosensors. Paper-based and PDMS are the ones broadly used for this fabrication process owing to their cost-effectiveness and time-efficient fabrication process (Khunger et al., 2021).

In addition, due to their real-time diagnosis and smaller sample volumes, LOC biosensors have other benefits, such as rapid testing and response times, ease of handling, and sensitivity to standard analytic procedures. However, they can be applied anywhere in any environmental interface without any hurdles. In addition, LOC biosensors generally rely on proteomics, cell biology and microbiology applications. In proteomics, these devices exhibit the excellent potential to integrate the all-proteomics phases beginning from (1) extraction, (2) separation, (3) electrophoresis, (4) mass spectroscopy evaluation and (5) protein crystallization (Ansari and Malhotra, 2022; Verma and Bhardwaj, 2015). Similarly, cell biology copes with the vast number of cells in seconds because they can optimize all large quantity cells at the mono-level. Due to this, it can easily detect, sort out and isolate a single quantified cell when programmed. Whereas, for molecular biology, this is the quickest way of PCR detection by testing the excellent speed μ-scale thermal shift. Due to this, DNA array can be detected more than a million times rapid genome arrangement (Chakraborty et al., 2018; Dwivedi et al., 2021; Ho et al., 2021; Lei et al., 2019; Naguib et al., 2021; Novoselov et al., 2004; Patel et al., 2016; Solanki et al., 2011; Wu et al., 2022; Zhang et al., 2022). However, this generation's sensors are unable to incorporate present-day intelligent technological advancements and innovations.

Furthermore, LOC architect possess different substrate and packaging strutcures, including thread, film, paper, electronic chips, and other prominent flexible substrates, with applications in point-of-care diagnosing diversified pathogens. For instance, Choi et al. (Choi, 2020) summarized the various point-of-care biosensors for diagnosing severe acute respiratory syndrome coronavirus 2 (SARS-CoV-2) architected using various substrates, nanomaterials and packaging modules (Fig. 3).

Further, the emergence of artificial intelligence (AI), bioinformatics, data clouding and 5G communications in biomedical sectors have transformed the LOC module biosensors into 5th generation biosensors with smart, remote and intelligent prospects (Jin et al., 2020; Kim et al., 2019; Singh et al., 2021; Xin et al., 2020). Moreover, incorporating the fundamentals of triboelectricity for self-powered module biosensors and the fundamentals of green chemistry(Batra et al., 2022; Chaudhary, 2022) to address ecological concerns resulting in repurpose, reuse, degradable, recyclable biosensors, addressed under 5th generation of biosensors (Chaudhary et al., 2022c; Kim et al., 2020; Pathania et al., 2022). Therefore, it has raised the paradigm of intelligent, eco-friendly, and remotely accessible biosensors, whose utilization is not only limited to analyte monitoring but extended to advanced deliverables, including drug delivery, curable tactics, prevention functionality, antipathogenic activities and telemedicine. Additionally, the world is shifting towards 6G-IoT networks of ultra-reliable and low latency communications (URLLC) and enhanced mobile broadband (eMBB) at a significant pace (Nayak et al., 2020; Nguyen et al., 2022). Their integration into 5th generation modules further possesses the potential to revolutionize healthcare with real-time features like holographic communication and remote surgery. Therefore, it prompts the advancement towards 6th generation on-site biosensors. However, their development is in its infancy and requires extensive research and dedication, which has kept the current focus of research on 5th generation of biosensors.

2. State-of-the-art 5th generation biosensors: towards hospital-on-chip module

The state-of-the-art 5th generation biosensors are concerned with exploring advanced nanomaterials as sensing platforms, interfacing them with rapid and intelligent data processing strategies, and packing them in portable and wearable modules for diversified healthcare applications. The two major research concerns of 5th generation biosensors are dedicated to achieving utmost efficacy with stable performance and multi-functionality with the integration of other cutting-edge technologies (Chaudhary et al., 2022c).

The first concern related to 5th generation biosensors is catered by

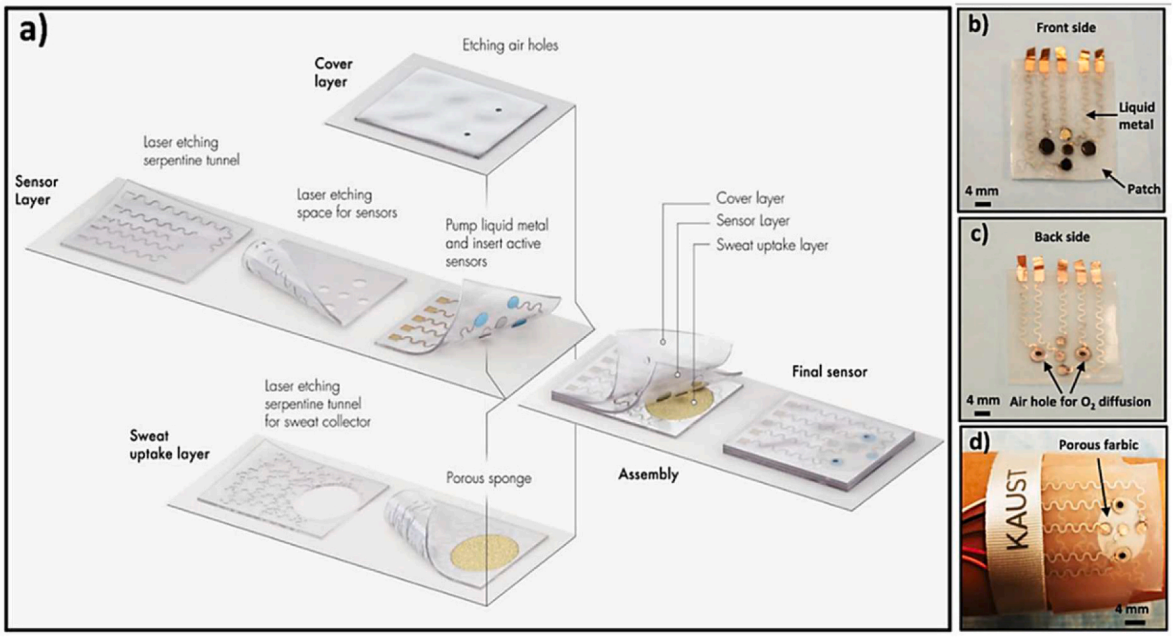

Fig. 4. Schematic illustration of the MXene-based biosensor system based on a lab-on-chip module for sweat detection (Lei et al., 2019).

architecting advanced functional nanoplatforms and engineering their physicochemical attributes. Recently, two-dimensional (2D) nanomaterials, including graphene and its derivatives, metal carbides and nitrides (MXenes), metal borides (MBenes), metal-organic framework, metal dichalcogenides and borophene, due to their high specific surface area have emerged as excellent biosensing platforms with enhanced detection and monitoring efficacies (Ahmed et al., 2020; Chakraborty et al., 2018; Chaudhary et al., 2022e, 2022a; Dwivedi et al., 2021; Ho et al., 2021; Huang et al., 2020; Jiang et al., 2020; Naguib et al., 2021; Wu et al., 2022; Zha et al., 2019; Zhang et al., 2022) Amongst all, MXenes have demonstrated enormous potential in detecting and monitoring the diversified biomolecules utilizing various strategies, encompassing electrical, electronic, electrochemical, optical, acoustic and plasmonic modules (Chaudhary et al., 2022a, 2022c, 2022e; Sheth et al., 2022). It is attributed to the high effective surface area, tunable physicochemical attributes, and rich surface functionalities of MXenes, which contribute to enhanced monitoring performances. Moreover, their hybridization and intercalation with foreign nanomaterials cater to difficulties associated with new MXene-based biosensors of poor stability due to oxidation and restacking of layers(Alwarappan et al., 2022). For instance, Lei et al. (2019) fabricated the electrochemical biosensors for the in-vitro perspiration investigation. Then, they applied the multifunctional and wearable sensor prepared via MXene-composite with Prussian blue for the sensitive, curable, and durable tracking of lactate and glucose present in sweat, as illustrated in Fig. 4. This further helps to enhance the linear detection and accuracy rate to prevent personalized health issues and early-life diseases. This progress of on-site solution based MXene biosensors has been further supported by numerous reports in the literature, as detailed in this review.

Moreover, the sudden outbreak of fatal and infectious diseases has overwhelmed the existing global healthcare services and resulted in increased severity and mortalities, raising a second concern related to 5^{th} generation biosensor's architecture and packaging. Nowadays, especially in the current coronavirus disease (COVID-19) scenario, the primary global health concern is early diagnosis, which strengthens the treatment efficacies and curtails the associated severity and mortality (Chaudhary et al., 2022b; Kaushik et al., 2020; Noh et al., 2022). These consequences can be controlled through early diagnosis of respective biomarkers/pathogens, thereby enhancing therapeutic efficiency, and developing personalized intelligent healthcare equipment(Cherusseri et al., 2022; Markandan et al., 2022). Furthermore, it has raised the paradigm of compact, portable, multi-functional and solution-providing biosensors with hospital-on-chip (HOC) modules to provide healthcare access to every individual, even in the remotest part (Kaushik et al.,

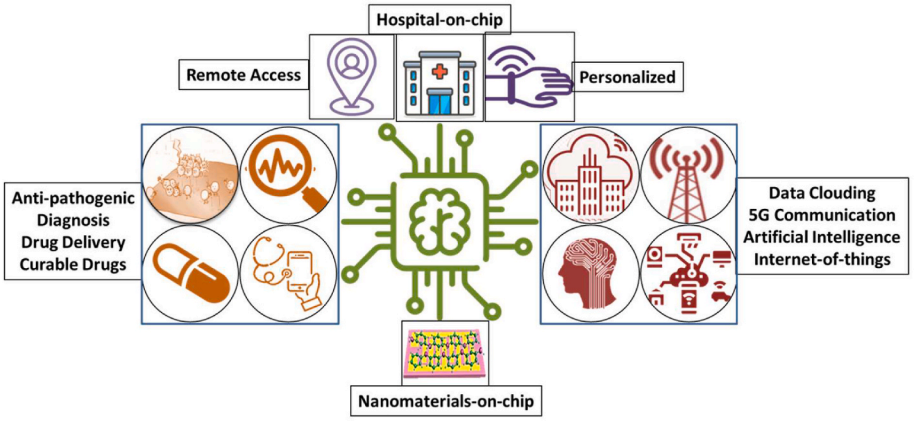

Fig. 5. Hospital-on-chip module-based 5th generation of compact, portable, and intelligent biosensors.

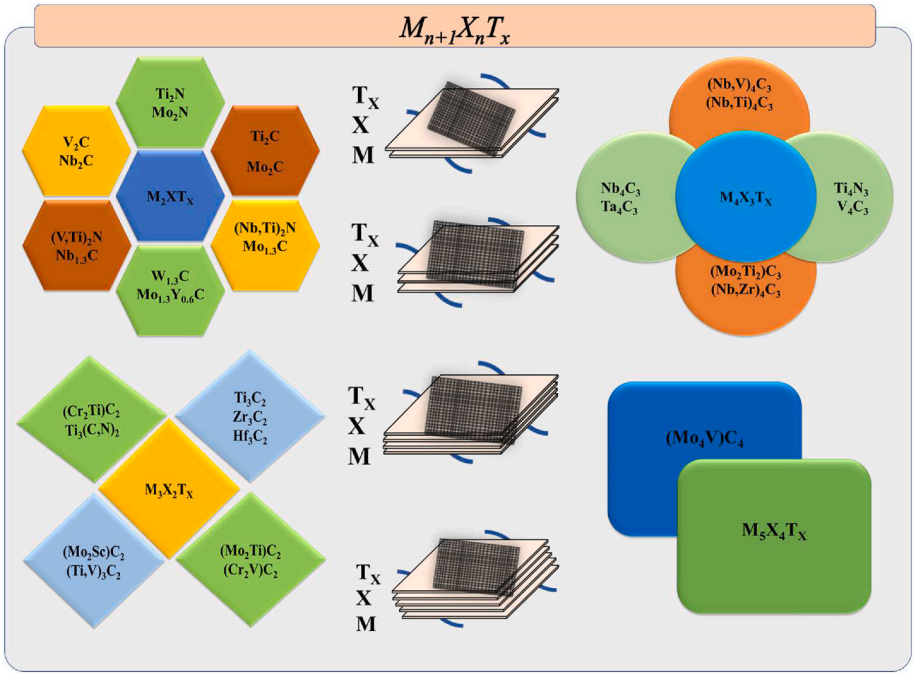

Fig. 6. Expanding family of MXenes classified based on numbers of layers, stoichiometry, and surface functionalities, displaying all MXene classes grouped by layer count.

2015; Tiwari et al., 2019). The importance of HOC biosensors lies in their diversified advantages and multifunctionality of diagnosis, imaging, monitoring, sensing, telemedicine, drug release and antipathogenic action embedded in a single chip with prospects of remote access and personalized healthcare serving the sustainable development goals (Fig. 5).

Moreover, these biosensors integrated into smart IoTs perform multifunction, including non-invasive monitoring of various health parameters of the human body simultaneously (Chaudhary et al., 2022a, 2022c). The research and development of biosensors are dedicated to the prompt and accurate monitoring of biomarkers/biochemicals in the human body due to biological imbalances resulting from chronic diseases(Gautam, 2022; Ghosh et al., 2022; Markandan et al., 2022). Furthermore, designing compact and portable modules, especially during COVID-19, has emerged as a massive, personalized healthcare need to protect against the spread of contagion from infected to non-infected individuals (Chaudhary et al., 2022b; Pathania et al., 2022). It has raised the burden on the global wearable and personalized healthcare market due to the requirement of remote and individual access to healthcare diagnostic facilities.

Hence, this paradigm has recently shifted from LOC to HOC modules due to the emergent requirements of on-site healthcare diagnostics and their solutions. Nowadays, it is becoming the scalable solution for the requirement of any family and extensively for the “doctor house call”, which made this possible virtually to every place within no time limit. Most importantly, this was necessarily thinkable because of the availability of mobile internet, broadband and other wireless technology for telemedicine and remedy decision aids (Jin et al., 2020; Verma et al., 2022). Similarly, to be thorough and effective, technologies for diagnosing and treating various household diseases must be available as soon as possible. In addition, this can be completed by healthier lifestyles, a clean environment and smart web sensors. Therefore, researchers are now implementing intelligent 5th generation biosensors to protect precious life from these dangerous diseases (Lei et al., 2019; Li et al., 2022; Novoselov et al., 2004; Pan et al., 2022; Patel et al., 2016; Solanki et al., 2011; Verma and Bhardwaj, 2015).

This review comprehensively discusses the MXene-based various kinds of intelligent biosensors with on-site and point-of-care modules and their journey toward LOC and HOC biosensors. This review highlights the state-of-the-art MXene fabrication, advancements in its physicochemical attributes, diversified 5th generation biosensing modules and applications, and intelligent prospects to design HOC strategies. Besides, it discusses the challenges related to the practical development and commercialization of MXene-based on-site biosensor modules and their possible alternate solutions with innovative intelligent prospects.

3. Engineering MXenes-based materials to architect future-generation biosensors

Since the extraction of monolayer graphene sheets from monolithic graphite in 2004, two-dimensional (2D) materials have gained much attention. The 2D substances are usually thin atomic mono-layers of 5–10 nm thickness or a few numbers of thin layers coupled by van-der Waals (vdW) interactions (Dwivedi et al., 2021). Due to its linear electronic dispersion, graphene and its distinct forms, such as reduced graphene oxide (rGO), graphene nanoplatelets (GNPs) and graphene oxide (GO), have been the most thoroughly investigated 2D materials to date, with substantial progress toward commercialization (Wu et al., 2022; Zhang et al., 2022). However, in 2D materials, where vdW forces may segregate an atomically thin layer from bulk material, they are only the tip of the iceberg. In recent years, novel vdW 2D nanostructured future-generation materials, such as MXenes, have emerged, with similar physicochemical behavior to graphene and its derivatives and the added benefits of hydrophilic nature, high stability, accessible to functionalization, increased flake size, improved yield, and better machine processability (Chakraborty et al., 2018; Ho et al., 2021; Naguib et al., 2021). These 2D materials have diverse surface compositions, adjustable interlayer spacing, and physicochemical properties that may be optimized, making them ideal alternatives for developing advanced future-generation sensors. Most investigations have been dedicated to designing their structure and optimizing their characteristics by regulating the interaction factors, modifying interlayer spacing, exploring stoichiometry, and tuning and functionalizing the surface.

2D MXenes, ever since their inception in 2011, has attracted extensive research interest across all 2D materials (Huang et al., 2020; Jiang et al., 2020; Naguib et al., 2021). MXenes are a newly developed family

Table 1
A comprehensive summary of diversified MXene's fabrication strategies resulting in different surface terminations using a top-down strategy comprised of selective etching from different precursors (Chakraborty et al., 2018; Chaudhary et al., 2022c; Ho et al., 2021; Jiang et al., 2020; Naguib et al., 2021; Wei et al., 2021).

MAX Phases	Etched MXene	Etchant Used	Etchant Strategy	Surface Termination Group
Ti_3AlC_2, V_2AlC, Nb_2AlC, Nb_4AlC_3, Ta_4AlC_3, $(Ti,Nb)_2AlC$, $Mo_2Ti_2AlC_3$, $Mo_2Ga_2C_2T_x$, $Hf_3(AlSi)_4C_6$, $Zr_3Al_3C_5$ $(Mo_{2/3}Sc_{1/3})_2AlC$	$Ti_3C_2T_x$, V_2CT_x, Nb_2CT_x, $Nb_4C_3T_x$, $Ta_4C_3T_x$, $(Ti,Nb)_2CT_x$, $Mo_2Ti_2C_3T_x$, Mo_2C, $Hf_3C_2T_x$, $Zr_3C_2T_x$ $Mo_{1.33}CT_x$	HF	HF etching	-O, –OH, –F
Ti_2AlC, Ti_3AlC_2, $(Nb,Zr)_4AlC_3$, V_2AlC, Ti_3AlCN	Ti_2CT_x, $Ti_3C_2T_x$, $(Nb,Zr)_4C_3T_x$, V_2CTx, Ti_3CNT_x	LiF/KF/NaF/FeF_3/NH_4F + HCl, $NaHF_2$/KHF_2/NH_4HF_2; LiF/KF/NaF/FeF_3/NH_4F + HCl; NH_4F + $C_5H_{14}Cl$ $H_2C_2O_4$; Ionic liquid ($EMIMBF_4$/$BMIMPF_6$), LiF + HCl, NaF + HCl, LiF + HCl	In situ HF formation etching	-O, –OH, –F -O, –F (ionic liquid)
Ti_3AlC_2	$Ti_3C_2T_x$,	NaOH + H_2SO_4, NaOH, KOH	Alkali etching	-OH, –O
Ti_3AlC_2, V_2AlC, Cr_2AlC	$Ti_3C_2T_x$, V_2CT_x, Cr_2CT_x	NH_4Cl + TMAOH/HCl, HCl, HCl	Electrochemical Etching	-OH, –O, -Cl
Ti_3SiC_2,Ti_3ZnC_2 Ti_4AlN_3	$Ti_3C_2T_x$ $Ti_4N_3T_x$	$CuCl_2$, $FeCl_2$/$CoCl_2$/$NiCl_2$/$AgCl_2$/$CdCl_2$ KF/LiF/NaF	Molten salt etching	-O, -Cl -O, –F
Ti_3AlC_2	$Ti_3C_2T_x$	I_2	Etching	-O, –OH, –I
Mo_2Ga_2C	Mo_2C	Ultraviolet light (100W)	UV	-O
Ti_3AlC_2	$Ti_3C_2T_x$	LiF	Surface acoustic waves (SAWs)	-O, –OH, –F
Ti_2SC	Ti_2CT_x	400–900 °C	Thermal reduction Strategy	-O, –OH
Ti_3AlC_2	$Ti_3C_2T_x$	Algae	Bioreduction	-O, –OH

of 2D layered transitional metallic nitrides/carbides/carbonitrides elucidated by $M_{n+1}X_nT_x$, where 'n' signifies layers, number bonded together through vdW forces, 'M' denotes initial transitional metals (e.g., Ti, Mo, Sc and V). 'X' stands for nitrogen/carbon/carbonitrides, and 'T' refers to the surface terminals groups, i.e., oxygen (-O), chlorine (-Cl), fluorine (-F) and hydroxyl (-OH) (Naguib et al., 2021). The 'M' atoms in the double transition metal MXene can be found in either an arranged or randomized phase of solid solution, with an ordered arrangement being far more energetically stable (Jiang et al., 2020; Naguib et al., 2021). MXenes family is continuously growing due to the development of a myriad of synthetic MXenes together with varied stoichiometry, including $Ti_3C_2T_x$, Ti_3CNT_x, and $(Ti_{0.5}Nb_{0.5})_2CT_x$, as shown in Fig. 6.

Similarly, the number of etching strategies, such as 3D 'MAX' ($M_{n+1}AX_n$, where A is 13/14 group element) (Jiang et al., 2020; Naguib et al., 2021), 'non-MAX' [14], i.e., $(MC)_n$ $[Al(A)]_mC_{(m-1)}$, where m is 3,4, and A is Si or Ge and 'modified-MAX' with 'i-max phase,' i.e., $(M^1_{2/3}M^2_{1/3})_2AX$) have been utilized to develop MXenes (Chaudhary et al., 2022c). A Multi-layered MXene is produced after removing the layers of 'A/A-C' from its original precursor's form (Jiang et al., 2020; Naguib et al., 2021). Therefore, with the applications of modern computational methodologies based on a detailed electronic structure and phonon analyses, a verified, more detailed image of the potential of eliminating the middle layer (A/A-C) out of the precursor to produce MXene was assessed theoretically (Jiang et al., 2020). For example, to envision the exfoliating and etching prospects of 82 MAX precursors, the static-exfoliation energies were predicted using force constants (Khazaei et al., 2013). The findings demonstrated that projected average force constants for 'A' atoms within precursors were in linear relation with the exfoliation perspective, revealing that eliminating 'A' layers may form MXene.

To extract and develop the MXene layer from its respective precursors, chemical methods comprising two primary phases, namely selective etching and delamination, were applied in the experimental investigation (Huang et al., 2020; Naguib et al., 2021). In contrast, numerous etching techniques segregate the middle layers of 'A/A-C/A-l-A-C' from the precursor for producing the MXene sheet (Naguib et al., 2021). These approaches tend to etch MXene layers, encompassing fluorine-carrying etchants (e.g. HF, LiF and HCl mixture, fluorine-incorporated liquefied salt, and fluoride salts), non-fluorinated etching, such as electrochemistry and alkaline rich hydrothermal etching process, and non-aqueous liquid phased etching method employing Lewis acidic salts (Jiang et al., 2020; Naguib et al., 2021). To illustrate this, Naguib et al. (2011) disclosed the initial production of $Ti_3C_2T_X$-based MXene from its respective Ti_3AlC_2 MAX precursor through selective HF etching of 'Al'. Molecular dynamic ab-initio-based computing simulations show that the structural bonding of Ti–Al degrades significantly when the radicals F/H from the adsorbed HF are decomposed over Ti atoms, resulting in surface functionalities and the formation of $Ti_3C_2T_X$. Following this, ample etching techniques have been devised to construct distinct MXenes, as illustrated in Table 1.

A selective etching process is usually a kinetically controlled process in which the emergence of surface functionalities onto the MXene surface is governed by the precise etching method and reaction environment (Table 1). Fluorine-based etchants, for example, lead to surface terminations of –F, –OH and –O. While etching process without fluorine eliminates fluorine surface functions from MXenes (Khaledialidusti et al., 2020; Q. Li et al., 2021). Mono-layered MXene sheets could be produced successfully through a suitable delamination approach that may depend on the type of surface functions occurring within multi-layer MXene. To illustrate, the emergence of oxygen-based functional groups leads to highly critical interlayer bonding. While the active hydroxide (-OH) groups are more likely to deform the MXene layers (Wei et al., 2021). Ion intercalation may readily delaminate several layer MXenes, extending the interlayer gap of multilayer MXenes. The intercalation process incorporates intercalation compounds, i.e., dimethyl sulfoxide (DMSO) and tetrabutylammonium hydroxide (TBAOH), metal cations, and secondary nanofillers, such as macromolecules (Wei et al., 2021). In this section, the strategies evolved to produce diversified MXenes utilizing selective etching have been reviewed comprehensively (Jiang et al., 2020; Naguib et al., 2021; Wei et al., 2021). A rigorous description of MXene manufacturing utilizing multiple precursors and etching techniques is presented in Table 1.

Nevertheless, the physicochemical properties and application efficacy of these mechanically stimulated MXenes get influenced due to the presence of several defects (Naguib et al., 2021). Further, harmful, and volatile HF etchant, along with other etchants, causes environmental pollutants and threatens users' safety and health. Consequently, numerous bottom-up techniques for MXene production have been explored, including atomic layer deposition, chemical vapor deposition, and plasma-enhanced pulsed laser deposition (PEPLD) (Aghamohammadi et al., 2021; Naguib et al., 2021; Wei et al., 2021). Gogotsi

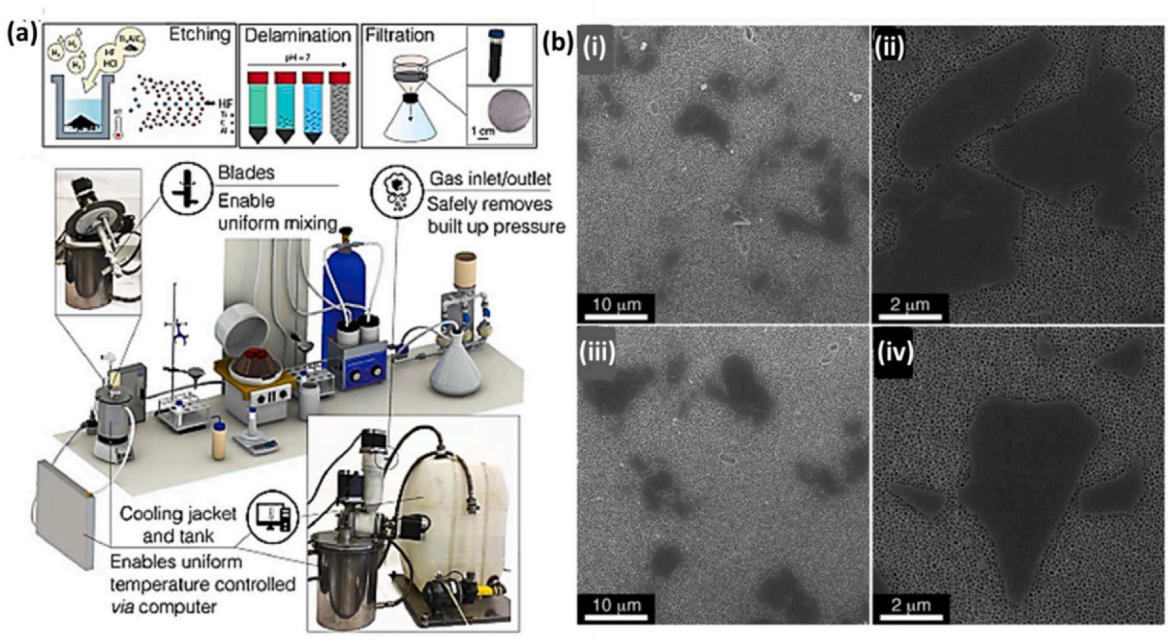

Fig. 7. Illustration of scalable fabrication strategy for manufacturing MXenes in (a) A large reactor with cooling provisions, and (b) Morphological analysis based comparison between MXenes prepared through small traditional chemical strategy and large scale reactor (Shuck et al., 2020).

et al. (Gogotsi, 2015) reported the bi-layer substrate of copper, which was reduced onto molybdenum foil having a size of ~100 μm to form molybdenum carbide crystal (Mo_2C) with ultrathin size by maintaining it at ~1085 °C with a low methane content. Even though these approaches hinder secondary contamination and user-related threats, they are very complicated, costly, time-consuming, and low-yielding methods. This not only limits their commercialism but also enforces to use of top-bottom approaches based on etchants for scaling MXene production.

Moreover, for commercializing and carrying technology from laboratories to the appropriate marketplaces, scalable production of MXenes is vital. The stumbling blocks in scalable manufacturing of MXene are controlling reactor capacity, persistent transfer and homogenous blending of precursors, regulating thermal reactions and preserving safety considerations, and achieving optimal reaction parameters to attain required physicochemical attributes (Naguib et al., 2021; Shuck et al., 2020; Wei et al., 2021; Zhao et al., 2019) Shuck et al. (2020) described the scalable manufacturing of MXene based on titanium carbide in a customized, large-scale chemical reactor with many necessities, such as cooling jackets, gas inlet and outlet with a screw feeding system, blender, temperature sensor and agitator for addressing the issues (Fig. 7(a)). The HF-based selective etching throughout the processing yielded multilayer $Ti_3C_2T_x$ MXene and mono-flake MXene. Later these materials were intercalated in a dried vacuum and water. In comparison, formation (etching utilizing traditional in-laboratory HF technique) of a large-size batch to that of the small-size batch was remarkably higher by 52%, with comparable physicochemical properties, showing the approach's effectiveness for mass manufacturing. Subsequently, the obtained MXene sheets were either several layered or few-layered after intercalating using water (Fig. 7(b: i-iv)) (Shuck et al., 2020). It necessitated a scalable intercalation process to achieve MXene with fewer layers or a single-layer arrangement.

Furthermore, Zhang et al. (S. J. Zhang et al., 2020) described a novel method to use an ammonium ion to address the problems related to the adhesion and reassembly of few-layer MXenes on a vast scale. To intercalate and delaminate the MXenes layers with a usual processing method, a solution-form-flocculation technique and redesigned method was implemented. This technique can scale up the production of numerable MXenes, such as $Ti_3C_2T_x$, $Nb_4C_3T_x$, V_2CT_x, Nb_2CT_x, and others. On the other hand, this method has been used merely to investigate $M_3C_2T_x$-MXene. This technique is yet to examine other related configurations of MXenes or synthesized MXenes. Additionally, several concerns, such as secondary environmental degradation and safety and health risks linked with the suggested scale-up processing, necessitate redesigning a more sustainable MXene production process at the commercial level.

4. Novel characteristics of MXenes-based materials for efficient biosensing

Optimizing the material's unique physicochemical attributes is the key to obtaining outstanding quality and fulfilling industrial material demands for the targeted application (Chaudhary, 2021a, 2022; Chaudhary et al., 2017, 2022a; Chaudhary and Chavali, 2021; Chaudhary and Kaur, 2015). It implies improvements in the detection material's physicochemical traits, which may be achieved during the manufacturing phase by optimizing the reaction conditions. Similarly, MXenes display outstanding physicochemical properties, such as hydrophilicity, flexibility, high mechanical durability, adjustable band gaps, rich surface chemistries, and huge active surface area (Wang et al., 2021; Weng et al., 2015) This makes MXenes a highly suitable material for designing next-generation sensors exhibiting excellent selectivity and sensitivity, biocompatibility as well as simple machine processability. However, by designing and developing hybrids/nanocomposites with other substances, various challenges associated with particular 2D materials can be addressed further (Chaudhary et al., 2021a; Dhall et al., 2021; Hashtroudi et al., 2020).

Usually, the physicochemical properties of MXenes are strongly influenced by their stoichiometry, interlayer spacing, specific size, layer numbers, and pattern for stacking. To exemplify, during the segregation of the A/A-C layer from its respective precursors, the 'M' ions become exposed on the faces of the MXenes layer (Wei et al., 2021). In the MXene sheet, these surfaced 'M' atoms are not only unstable but also highly prone to bonding with surface functional groups, such as –F, –OH, –O, and -Cl, which emerge from the etching processes and reduces the overall surface efficiency (Naguib et al., 2021; Wei et al., 2021). As a result, it becomes critical first to understand how T_x affects the physicochemical characteristics of MXenes sheets. So that better and

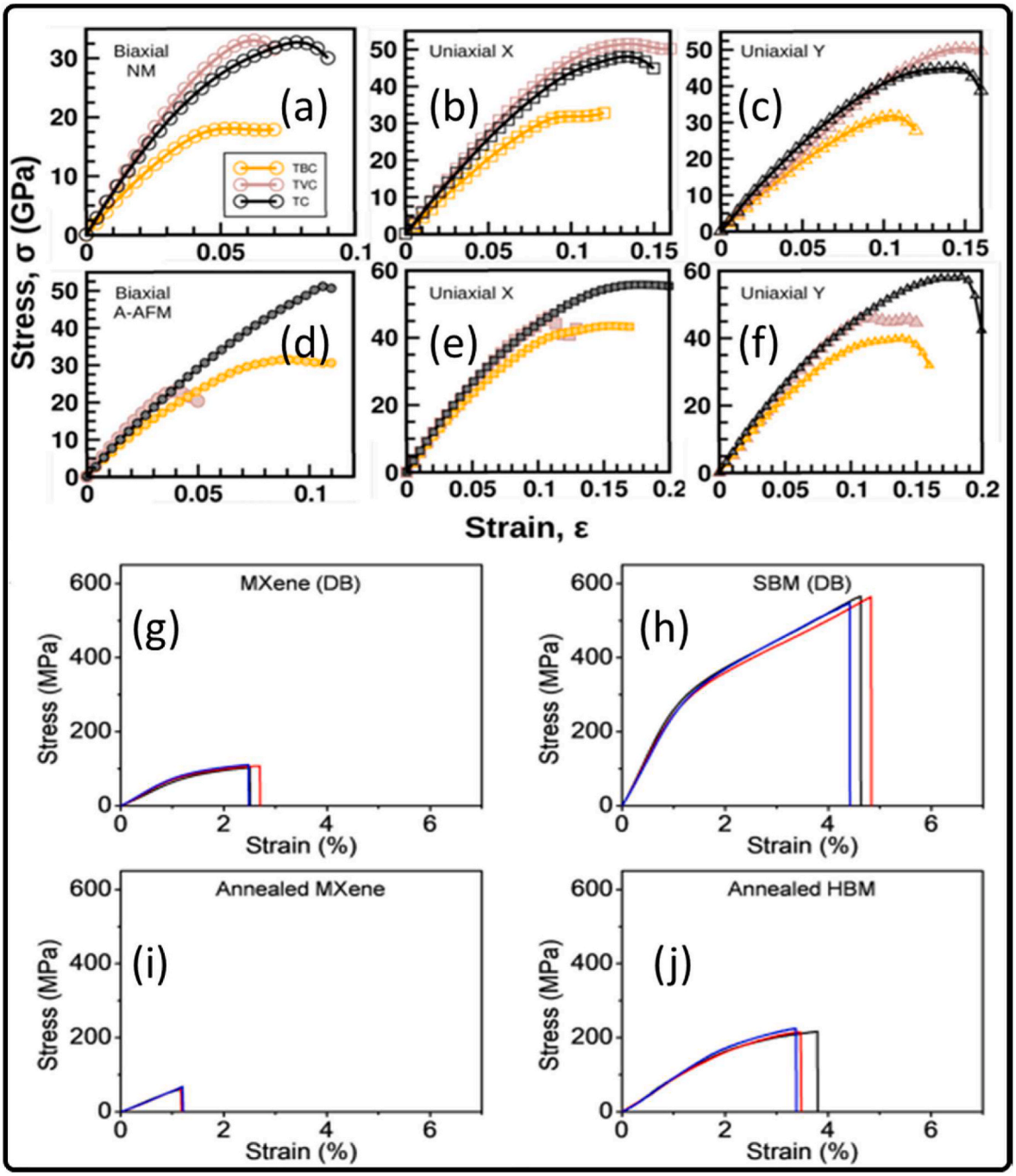

Fig. 8. Representing the stress and strain curves of the Ti_2C, $Ti_2(C_{0.5}B_{0.5})$ and (Ti, V) C under the uniaxial and biaxial tensile strength, also showing the outcomes of the antiferromagnetic and non-magnetic state (Chakraborty et al., 2018).

improved sensors can be designed. Apart from experimental validations, several computational programming based on advanced data learning techniques, such as machine learning (ML) and deep learning (DL) based on molecular dynamics (MD) or density-functional theory (DFT), have been predominantly used to analyze the changes in the physicochemical properties of MXenes in fluctuating and complex conditions.

4.1. Ambient and processing stability

For sensing applications, sensors must be thermally and chemically stable. The sensing material undergoes several chemical and heat treatments during machine processing for sensor manufacturing. After complete synthesis, it must perform efficiently in all operational conditions. Although MXene maintains its structural stability with saturated surface terminations, it is thermally unstable due to its stoichiometry due to the exposed 'M' atoms on both sides, which are unstable owing to weak interactions (Jiang et al., 2020). This enhances the nucleation growth of these exposed 'M' atoms when they react with water molecules or oxygen atoms, which then expand throughout the MXene, leading to structural defects with extended edges (Jiang et al., 2020; Zhan et al., 2020). It steadily accelerates MXene's oxidative disintegration into transition metal oxides. For example, in oxidative surroundings, such as heated temperatures, $Ti_3C_2T_x$ is unstable and gradually transforms into TiO_2 (He et al., 2021). These conversions may result in the loss of MXene's unique properties, including electrical and thermal conductance, hydrophilic nature, and increased

pseudo-capacitance, adversely affecting the projected sensor performance (Iqbal et al., 2021).

The production of oxidant-inhibitor MXenes employing sophisticated pre-processing and storing techniques cater to these stability limitations. These techniques consist of storage of MXene in inert conditions using gases, such as Ar for obstructing the effect of oxidation, storage at a low-temperature range to avoid nucleation propagation, preservation of MXene in organic or inorganic dispersions, cease edge atoms through absorption of anionic salts, and treat MXene with reduction gases (Chae et al., 2019; Lee et al., 2020; Natu et al., 2019; Zhang et al., 2017; Zhao et al., 2019). Also, designing MXene complex structures using carbon substances or macro-compounds or dispersing in ionic salted liquids have been proven strategies for an efficient antioxidant MXene (Chaudhary et al., 2021a; Du et al., 2021; Iqbal et al., 2021; Wu et al., 2017; Zhan et al., 2020). Further, treating MXene thermally at elevated temperatures (i.e., 1200 °C) in an argon environment eradicates surface terminations and enhances structural patterns without impairing layered microstructure (Wei et al., 2021). Therefore, the logical design of MXene-based products should be promoted for their intended uses.

Moreover, surface functionalization and hybridization are two important techniques essential to modulate interlayer spacing and preventing restacking of MXene layers and ambient oxidation. For instance, the introduction of macromolecules/polymer between the MXene layers prevents their restacking, providing stability, increases surface-to-volume ratio making MXene architect more accessible to analyte/biomolecule interaction, and modifies surface terminals to provide selectivity and stability. For instance, Li et al. (X. Li et al., 2020) described that the manifestation of dendritic polyaniline nanoparticles exfoliates the interlayer distance amongst the $Ti_3C_2T_x$ nanosheets in MXene/polymer hybrids. It considerably surges the specific surface area and porosity of MXene-hybrid, prompting it as a latent candidate for analyte detection. Moreover, the core-shell type morphology of Ti3C2Tx/PAN contributed to its ambient stability. Furthermore, Chen et al. (2020) reported the surge in surface area of DL-tartaric acid (DLTA) assembled $Ti_3C_2T_x$-MXene (less than 5 m^2/g) with the hybridization with polyaniline (20–23 m^2/g). Besides, the hybrid was reported to be mesoporous possessing broad pore-size distributions varying from 2 to 40 nm, which expedite the rapid analyte/ion/biomolecule diffusion and is highly favourable for biosensing applications

4.2. Machine processability

Optimizing materials' flexibility and mechanical strength in terms of tribological properties to fabricate next-generation sensors is indispensable. MXenes exhibit unique tribological properties that may be improved and optimized using numerous techniques. In a bi-layer $Ti_3C_2T_x$, for example, the young's modulus and elasticity observed were 502 GPa and ~655 N/m, respectively. This implies the improved interlayer association among surface functionalities (Borysiuk et al., 2015). Further, nanoindentation findings indicated that the elasticity of a bi-layer $Ti_3C_2T_x$ is far more significant than other two-dimensional materials such as GO, rGO, and MoS_2. Chakraborty et al. (2018) reported the mechanical properties and doping effect of Ti_2C MXene. As illustrated in Fig. 8, stress and strain relation possesses the lowest energy antiferromagnetic and non-magnetic states. It can be observed from the figure that there is a 25–27% decline in Young's modulus and plane stiffness of the $Ti_2(C_{0.5}B_{0.5})$ comparable to the MXene. Moreover, titanium doping over the V sites produced the undoped stiffness of MXene. In contrast, the calculated stiffness of $Ti_2(C_{0.5}B_{0.5})$ was noted to be 4.2, 1.5, 1.86 and 3.1, which is much greater than the stiffness of graphene, h-BN, MoS_2 and SiC, respectively.

Flexibility in sensor architecture can further be attained by developing self-sustained flexible thin films or using flexible substrates. For example, numerous MXenes, such as $Ti_3C_2T_x$, display a high degree of intrinsic flexibility when transformed into a conical design with a radius smaller than 20 nm (Naguib et al., 2011). To illustrate, self-standing $Ti_3C_2T_x$ thin films of approximately 3.3 μm thickness have mechanical strength of ~22 MPa. While $Ti_3C_2T_x$ cylindrically rolled paper of ~5 μm thickness showed sustainability over 4000 times its weight (Lipatov et al., 2018).

Moreover, there have been reports on scalable manufacturing of freestanding MXene Films with optimized flexibility utilizing distinct processes, such as sedimentation, membrane filtering, powder-coating, doctor blading, drop casting in a vacuum, and LBL assembly (Qian et al., 2022; Verma et al., 2022; J. S. Zhang et al., 2020; M. Q. Zhao et al., 2019). To illustrate, Lipton et al. (2020) demonstrated using an inverse-drop casting process to fabricate a scalable conductive and free-standing film of $Ti_3C_2T_x$ on a water-insoluble plastic substrate. Interestingly, self-standing MXene thin films are free of voids, which otherwise appear during conventional manufacturing.

Furthermore, Wan et al. (2021) have demonstrated a unique bridging-induced densification process for scalable production of MXene films. During synthesis, the layered structure of MXene was densified, and the voids were filled with a sequential mixture of covalent and hydrogen bonding molecules. Also, MXenes can be readily deposited on flexible substrate surfaces due to their outstanding dispersibility and hydrophilicity. Developing complex/hybrid MXene layers using macromolecules can also increase their flexibility (Chaudhary et al., 2021a). However, retaining the flexible nature and mechanical endurance of such complex MXenes throughout the machining process is exceptionally tedious. Still, it can be achieved through optimal precursor parameters like concentration during machine processing. Zhao et al. (Zhao et al., 2019) reported the flexible nature and the resilient character of $Ti_3C_2T_x$/CPAM HNC, which they attributed to CPAM's high affinity between the layers of $Ti_3C_2T_x$.

In contrast, Li et al. (Li et al., 2020) and Wang et al. (Wang et al., 2021a, 2021b) both groups successfully adopted the flexible Pl substrate surfaces to design flexible MXene-polymer hybrid gas sensing devices. Besides this, during etching with the emergence of hydrophilic functional elements, such as –O and –F, MXenes become highly dispersible to several solvents. The most common dispersion mediums for MXene are water, cyclic propylene carbonate, dimethyl sulfoxide, dimethylformamide, and a particular concentration of about 0.3 mg m/L of non-ionized solvents like toluene and hexane, which distinguishes it apart from other carbonaceous 2D nanomaterials including graphene and graphene-based derivatives. MXene's strong dispersion ability and hydrophilic nature enable their manufacturing by solution-based strategies, hybrid advances with other nanomaterials, and solution-processability to design sensing devices for numerous commercial applications.

4.3. Electronic and optical behavior

Electronic behavior, such as conductance and charge transfer, has become a critical underlying aspect in defining the target response of a sensing device application (Chaudhary, 2021b; Chaudhary et al., 2022a; Chaudhary and Chavali, 2021). For example, a polymer with 1D charge transfer routes detects stimulus variations more efficiently than one with 3D charge carrier transports (Chaudhary, 2021a, 2022; Chaudhary et al., 2017). It has increased the demand for pre-analyzing the electrical behavior of materials before determining their uses. Several computer simulations have revealed that the metallic behavior of MXenes, and valency and electrical conduction band are extremely close to the Fermi energy level (Jiang et al., 2020; Naguib et al., 2021). Additionally, it is proposed that surface functionalization can tailor the electrical character of MXenes to the semiconducting range (Dillon et al., 2016; Si et al., 2016; Weng et al., 2015).

DFT computational analysis, for example, indicated that the appearance of –OH and –F surface functionalities transform the metallic form of $Ti_3C_2T_x$ into a semiconductor with a projected electronic band gap ranging between 0.05 eV and 0.1 eV, respectively. This curtails the

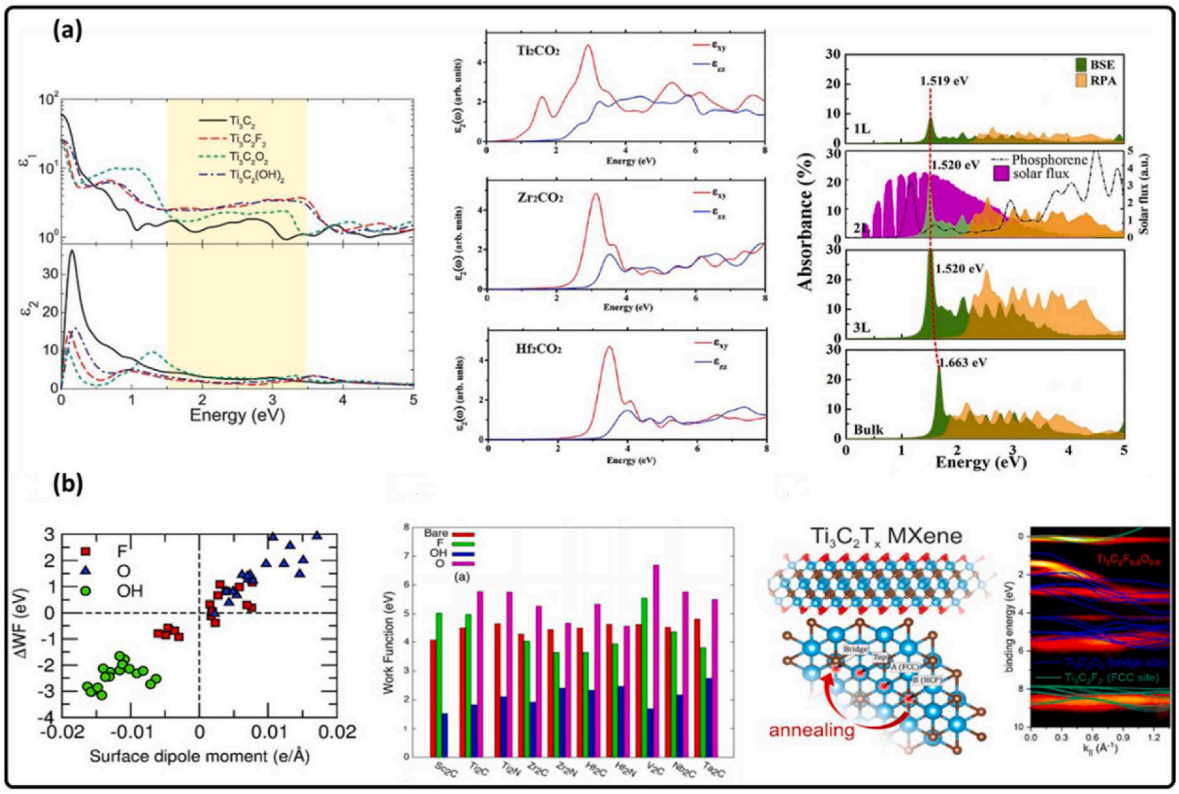

Fig. 9. Tunable electronic properties of Ti_2CT_x MXenes with diversified surface terminations analyzed through Density Functional Theory considering density of states (Berdiyorov, 2016).

electrical conductance of the material due to decreased charge transport density (Jiang et al., 2020; Xie and Kent, 2013). It has also been observed that changing the spatial arrangement of –F and –OH on MXenes leads to optical band gap modulation (Chakraborty et al., 2018; Jiang et al., 2020; Scott et al., 2022). As a result, by modifying the characteristics and geometric profile of functionalized surface groups, the electronic behavior of MXenes can be explicitly tailored for sensing applications. Also, MXenes' optical properties are intrinsically linked to their electrical character (Berdiyorov, 2016; Lashgari et al., 2014). DFT analysis revealed that most of the MXenes types, including $Ti_{n+1}X_n$, exhibit metallic properties because of the considerable overlap of the valence band and electrical conduction bands at the Fermi energy (Lashgari et al., 2014). Berdiyorov et al. (Berdiyorov, 2016) demonstrated the reliance of essential and unreal elements of frequency-assisted dielectric functionalities on surface elemental groups for numerous pure MXenes, such as Ti_3C_2, $Ti_3C_2F_2$, $Ti_3C_2O_2$, and $Ti_3C_2(OH)_2$. The electronic characteristics and densities of MXene are shown in Fig. 9.

Furthermore, the applicability of OH-reduced $Ti_3C_2T_X$ with lower reflection and absorption rate in the visible region makes it attractive for designing transparent and wearable electronic devices and photothermally targeted biosensing applications (Lei et al., 2020). Therefore, the tailorable electrical and optical behavior of MXene makes it a high potential material for designing the sensing devices of future-generation with sophisticated functions and high-performance outcomes.

5. Engineering advanced biosensors-based on MXenes-based materials

A biosensor is an analytical device that senses biological reactions by establishing distinct readout signals in response to interactions with biomes. It comprises two primary components: a physical-chemical converter and a biological receptor (Ansari and Malhotra, 2022; Chaudhary et al., 2022d). Because of their greater specific area and rapid charge transfer systems, one-dimensional (1D) nanomaterials, such as carbon nanotubes (CNTs), metal nanowires, and macromolecule nanofibers, have lately surpassed the obstacles related to typical biosensors based on bulk materials (Ansari and Malhotra, 2022; Zhou and Zhang, 2021). However, despite the remarkable biosensing performance of 1D materials, their costly production, erratic behavior in distinct device modules, and unstablility in varied environments have limited their commercial possibilities.

MXenes, on the other hand, offer more streamlined production competencies along with the ability to maintain physicochemical as well as electrical behavior along with rich surface functionalities, clearly making them highly intriguing for designing biosensing instruments (Ansari and Malhotra, 2022; Chaudhary et al., 2022d; Khunger et al., 2021; Zhou and Zhang, 2021). There have been several findings on 2D materials to form detectors or biomarkers for subjectively and quantitatively sensing metabolic abnormalities, evaluating the efficacy of various therapeutics, and assessing various environmental hazards such as infections and toxic substances. As per transducing reactions and sensing processes, a comprehensive classification of MXene-based biosensors has been discussed in this article (Table 2).

5.1. Advancements in electrochemical and electrical biosensors based on MXenes

The capability to sense biomes with a biosensor needs precise, vigilant, and targeted sensing for practical viability. The biosensors are designed according to the electrochemical modules for high sensitivity and selectivity of smaller biomolecules or biomes in the solution phase. MXenes, owing to rich electron-terminal surface chemistries that attract positively charged biomolecules, had been expected as attractive electrochemical biosensing receptors as well as transducers (Chaudhary et al., 2022e, 2022c; Shahzad et al., 2019; Sheth et al., 2022; Wu et al.,

Table 2
Summary of classes of various biosensor strategies for detection of various biomolecules and pathogens.

Type of Biosensor	Probing method	MXene Species	Target	Linear Detection Range	LOD	Ref.
Electrochemical	Screen-Printed electrode	$Ti_3C_2T_x$	Isoniazid and acetaminophen drugs	0.048 μM and 0.1–4.6 μM	0.064 μM	(Y. Zhang et al., 2019)
Electrochemical		$Ti_3C_2T_x$	Carbendazim (CBZ)	50–100 × 10^{-6}m	10.3 × 10^{-9}m	Wu et al., (2019)
Electrochemical		Nafion coated-$Ti_3C_2T_x$-modified-GCE	Dopamine	0.015–10 mM	3 nM	Shahzad et al., (2019)
Electrochemical	MXene based	MXene-Au-Pt	Superoxide molecule	0.4–9.5 × 10^{-6} M	0.2 × 10^{-6} M	Yao et al., (2020)
Electrochemical	MXene based	MXene/CNT/Prussian blue (PB) composite	Glucose Lactate	10 × 10^{-6}M to 1.5 × 10^{-3}M 0–22 × 10^{-3}M	0.33 × 10^{-6}M 0.67 × 10^{-6}M	Lei et al., (2019)
Electrochemical		MXene/Pt-NP/PAN composite	Lactate		5 × 10^{-6} M	Neampet et al., (2019)
Electrochemical		Pd@$Ti_3C_2T_x$ hybrid nanocomposite	L-Cys	0.5–10 μM	0.14 μM	Rasheed et al., (2019)
Electrochemical		$Ti_3C_2T_x$ MXene/graphite nanocomposite	Adrenaline		9.5 nM	No ref.
Electrochemical		$Ti_3C_2T_x$ MXene/layered double hydroxides (LDHs) composite	Glucose	0.002–4.096 mM		(M. Li et al., 2019)
Electrochemical		$Ti_3C_2T_x$ nanosheets	Mycotoxin	5 pM–10 pM	5 pM	Wang et al., (2019)
Electrochemical	capture hairpin probe (H1)	Ti_3AlC_2 MAX powder	microRNA-21 (miR-21)	m 100 fM to 100 nM	26 fM	Zhao et al., (2022)
Electrochemical	anionic redox	AuNPs/MXene@PAMAM, using 2D $Ti_3C_2T_\chi$	Human cardiac troponin T (cTnT)	0.1–1000 ng/mL	0.069 ng/mL	(X. X. Liu et al., 2022)
Dual-function Electrochemical		Urease enzyme immobilized MXene	Creatinine Urea	10–400 × 10^{-6} M 0–3 × 10^{-3} M	1.2 × 10^{-6} M 0.02 × 10^{-3} M	(J. Liu et al., 2019)
Dual-target Electrochemical	Dual-type Au microgap electrode	Aptamer/MXene (Ti_3C_2) nanosheet	Tumor necrosis factor α (TNF-α) interferon gamma (IFN-γ)	1 pg/mL to 10 ng/mL	0.25 pg/mL 0.26 pg/mL	Noh et al., (2022)
Field-Effect Transistor (FET)		Ti_2C MXene-graphene	SARS-CoV-2 2019-nCoV	25-250,000 copies/mL^{-1} 1-10 $pgmL^{-1}$	125copies/mL^{-1} 1FG mL^{-1}	(Y. Li et al., 2021)
Ratio-metric (Colorimetric)		Glutathione (GSH)–MXene QD composite	UA		125 × 10−9 M	Liu et al., (2020)
Colorimetric		MXene/CuS nanocomposite	cholesterol		1.9 × 10^{-6}M	(Y. Li et al., 2019)
Colorimetric		MXene/NiFe nanoflake composite	GSH	0.9–30 × 10^{-6} M	84 × 10^{-9}M	(H. Li et al., 2020)
Colorimetric/flurometric		N, P–Ti_3C_2 MXene quantum dots	Recognition of NO_2	1.5–80 μM	0.71 μM	Bai et al., (2022)
Colorimetric		Au/Pt/$Ti_3C_2Cl_2$ nanoflakes	Hydrogen peroxide (H2O2) Glutathione (GSH)	50–10000 μM 0.1–20 μM	10.24 μM 0.07 μM	Xi et al., (2022)
ECL	MXene-aptamer nanoprobes	MXene adsorbed exosome-cultured AuNP/PNIPAM/GCE	Breast cancer cell (MCF-7)	500–5000000particles per μL	~125particles per μL	(H. Zhang et al., 2019)
ECL		MXene/tris (4,4′-dicarboxyl-2,2′-bipyridine) ruthenium (II) ion (Ru (dcbpy)$_3^{2+}$) (an organic dye)/black phosphorus QD			37particles per μL	Fang et al., (2020)
ECL		MXene/Ru (dcbpy)$_3$ modified GCE	Single nucleotide mismatch in human urine	3fold superior ECL sensing response than whole matched nucleotides	1 × 10^{-9} M	Fang et al., (2018)
Photoelectrochemical		MXene QD	Glutathione		9 × 10^{-9} M	NO
Photoelectrochemical		2D Ti_2C	soluble CD146 (sCD146)	0.1–1000 pg/mL	18 fg/mL	Jiang et al., (2022)
Photoelectrochemical	MB sensitized MXene@ITO photoelectrodes	Label-free Ti_3C_2 MXene	Phosphorus	0.5–200 μM	0.21 μM	Chang et al., (2022)
Photoelectrochemical/ Electrochemical dual mode		Bi_2S_3/Ti_3C_2TX MXene nanocomposites	chlorogenic acid (CGA)	0.0282 μM–2824 μM (PEC sensor)	2.4 nM 43.1 nM	Qiu et al., (2022)

(*continued on next page*)

Table 2 (*continued*)

Type of Biosensor	Probing method	MXene Species	Target	Linear Detection Range	LOD	Ref.
				0.1412 μM–22.59 μM (EC sensor)		
ECL		PEI-Ru@Ti_3C_2@AuNPs composite	SARS-CoV-2 RdRp gene		12.8 aM	(K. Zhang et al., 2022)
ECL		Au@Ti_3C_2@PEI-Ru (dcbpy)$_3^{2+}$ hybrid nanocomposite	RNA-dependent RNA polymerase (RdRp) gene of SARS-CoV-2	1 fM-100pM	0.21 FM	Yao et al., (2021)
ECL	tetrahedral DNA/ aptamer cardiac troponin-I	Au/Ti_3C_2-MXene	Screening COVID-19	0.1 fM-1 pM to cTnI	0.04 FM	Mi et al., (2021)
ECL		Ru–$Ti_3C_2T_X$-AuNPs	DNA phosphorylated with polynucleotide kinase (PNK)	0.002–10 U mL139	0.0002 U mL139	(L. Wang et al., 2022)
ECL		2D Ti_3C_2 and CDS: W nanocrystals	MicroRNA-141	0.6 pM–4000 pM	0.26 pM	Du et al., (2022)

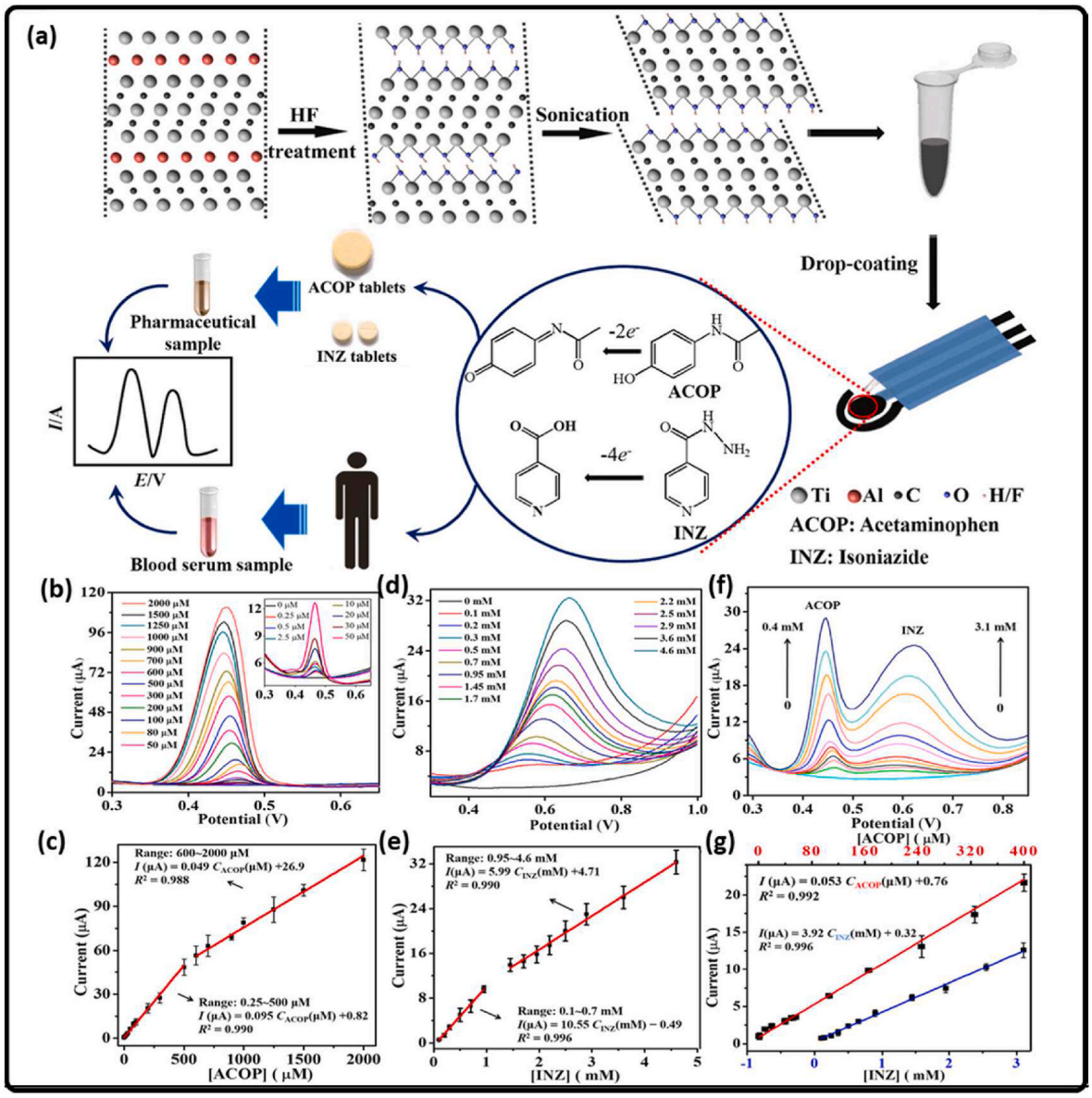

Fig. 10. (a) Schematic illustration of $Ti_3C_2T_x$ MXene processing and electrocatalytic oxidation mechanism with monitoring of ACOP and INZ by $Ti_3C_2T_x$-MXene/SPE and their Differential pulse voltammograms recorded for different concentration levels of ACOP (b) in INZ (c) in H_2SO_4 (0.1 M), and explored the dependence of peak currents with concentrations of ACOP, (d) of INZ (e) from 3 corresponding assessments, (f) GCE- $Ti_3C_2T_x$ -MXene in H2SO4 (0.1 M) with variable INZ and ACOP concentrations, (g) Recorded dependence of the peak current over the ACOP concentration (red line) and INZ concentration (blue line) while recording three corresponding assessments (Zhang et al., 2019).

2019; Yao et al., 2020; Zhang et al., 2019). Zhang et al. (Zhang et al., 2019) utilized $Ti_3C_2T_x$ nanosheets tuned screen-printed electrode (SPE) to identify two regularly utilized medicines, namely isoniazid (INZ) and acetaminophen (ACOP), which are known to cause liver problems in human beings. Linear sensing ranges for ACOP and INZ of 0.252000 M and 0.146 M, respectively, with 0.048 M and 0.064 M LODs, which were relatively higher than unmodified SPE, were observed by the detector (Fig. 10(a–g)). It has been ascribed to the abundant vacancies on the surface of MXene owing to the occurrence of functional groups, such as –F, –O and –OH on the surface.

Moreover, the observed high-performance of modified MXene/SPE electrode in INZ and ACOP detection to three attributes, including mechanical robustness and faster charge transport networks of MXene, accordion-like layered structure of MXene favoring more binding sites and felicitating charge carrier charge transport, and negatively charge surface of MXene due to its surface terminals favoring the aggregation of positively charged analytes.

In general, for biosensing applications, 2D materials can be easily functionalized with the polymer chain via non-covalent - π-π bond interaction (Chaudhary et al., 2021a, 2021b, 2022c; Gund et al., 2019). As a result, different antibodies can be coupled to these short-chain polymers in order to immobilize bacterial and targeted viral antigens with greater specificity for sensing evaluation. Moreover, the sensitivity progress of these 2D materials dramatically depends on the VdW types π-π bond interaction along with the chain polymers. Similarly, being non-covalently bonded, the functionalization mechanism needs the specific species of chemical groups in the chain reaction to induce lower signal-to-noise ratios whenever the bonding phenomena is weak or deficient. Therefore, utilizing the MXene because of the various functional groups (-F, –H, –OH) and excellent conductive nature, it can easily form a covalent bond with other materials, especially polymers. Hence, a large number of bioanalytes can be detected by modulating the surface terminals of MXenes (Chaudhary et al., 2022c; Ho et al., 2021; Noh et al., 2022).

Moreover, the interaction between various functional groups and analytes is specific and can be further optimized through hybridization. Therefore, it leads to selective detection of bioanalytes by tuning the surface terminals of MXenes as per targeted diagnosis/detection. Besides, the high conductivity of MXene provides better and faster charge carrier transport in hybrid-system based biosensing layers constituting a strong detection signal and resulting in high-performance diagnosis.

MXene ECL biosensors have also been widely used in sensing a range of bio-substances, such as antigens, carcinoembryonic, and dopamine. For example, Wu et al. (2019) used linear sensing ranged (50–100 × 10^{-6} m with a LOD of 10.3 × 10^{-9} m) $Ti_3C_2T_x$ based electrochemical biosensor to detect carbendazim (CBZ). They have also observed the exceptional selectivity efficacy of the designed sensor primarily because introducing other interfering analytes did not affect its sensing ability to CBZ. In addition, the surface functionalities of MXene with oxygen and fluorine terminals resulting in superior catalytic/electrocatalytic activities were ascribed to its high performance in detecting CBZ.

Similarly, Shahzad et al. (2019) described a Nafion coated- $Ti_3C_2T_x$ -advanced-GCE for sensing dopamine, having a sensing range of 0.01510 mM and a LOD of 3 nM. The electrostatic association between positive-charged dopamine atoms and oppositely charged $Ti_3C_2T_x$/Nafion was accredited to the improved dopamine sensing. It is also notable that secondary chemical additives in 2D layered materials can increase biosensors' targeting and sensitivity abilities. A superoxide ion, for instance, emerged during the antigen-antibody interaction and was identified through an electrochemical biosensing device based on MXene-Au-Pt nanoparticles (Yao et al., 2020). The biosensor depicted an excellent linear sensing range (0.4–9.5 × 10^{-6} M and a LOD 0.2 × 10^{-6} M) and selectivity owing to the secondary additives (Au and Pt NPS) of the MXene probe stimulated catalytic interactions throughout the detection phenomena. Additionally, the sensor's commercial viability was elucidated by employing in-vitro evaluations of zymosan feeding to the cells of Hep-G2. As a result, the designed sensor can sense a minimal concentration of the superoxide formed due to the inclusion of Hep-G2 in 5L of zymosan. These outcomes provided a green and efficient way to construct the outperforming MXene paper-based next-generation flexible biosensor by regulating growth mechanism and surface functionalities.

Several reports have described electrochemical biosensors based on secondary additive MXenes to detect numerous biomolecules, such as piroxicam, ascorbic acid, uric acid and ACOP (Chaudhary et al., 2022d; Khunger et al., 2021). In biological processes, enzymes act as catalysts and react with specific ligands. Therefore, to enhance the selectivity and sensing range of biosensors, ample ligand-enzyme interactions are carried out. As a result, electrochemical biosensing approaches rely on the sensing material's indirect response with the byproducts of the enzyme-analyte active engagement rather than directly reacting with the analytic substance (Kim et al., 2015; M. Li et al., 2019; Lin et al., 2020; Neampet et al., 2019; Rasheed et al., 2019; Wang et al., 2019) For instance, MXene/CNT/Prussian blue (PB) nanocomposite was used to design ECL biosensors to monitor glucose and lactate (Lei et al., 2019; Novoselov et al., 2004). Firstly, the sensor was tuned using oxidase enzymes of lactate and glucose that produced hydrogen peroxide and ionized the PB while interacting with each other. These generated ions begin reacting with the MXene probe, causing a redox reaction that increases the electrochemical sensing ability. The developed sensor exhibited a linear sensing range of 10 × 10^{-6} M to 1.5 × 10^{-3} M with 0.33 × 10^{-6} M LOD for glucose and a range of 0–22 × 10^{-3} M with LOD 0.67 × 10^{-6} M for detecting lactate. In a similar finding, Neampet et al. (2019) described the sensible detection of lactate using MXene/Pt-NP/PAN-based composite. The biosensor was gently tuned with lactate oxidase enzyme showing 5 × 10^{-6} M of LOD.

Moving further, surface chemistries and modifications help stabilize 2D nanomaterials for superior biosensing performance. For example, a hybrid Pd@$Ti_3C_2T_x$ nanocomposite sensor demonstrated electrochemical detection of L-Cys (Rasheed et al., 2019). The hybrid sensor also maintained a sensing range of approximately 0.5–10 μM and 0.14 μM of LOD linearly for L-Cys. Identically, a biosensor synthesized hybrid MXene/graphite $Ti_3C_2T_x$ nanocomposite monitored adrenaline electrochemically, having 9.5 nM of LOD. All the precursors of MXene-hybrids contributed to the enhanced detection of L-Cys. For instance, $Ti_3C_2T_x$ exhibited reducing action at the electrode surface and acts as an active conductive matrix for charge transport, while Pd NPs enhanced the ambient stability of MXene and the electrocatalytic activity of hybrid towards L-Cys monitoring.

In addition, Li et al. (Li et al., 2019) demonstrated the detection of non-enzymatic glucose with a linear sensing range of 0.002–4.096 mM with the application of a $Ti_3C_2T_x$ MXene/double layered hydroxides (LDHs) sensor. This sensing mechanism is primarily due to the glucose oxidation onto Ni–Co-LDH in an alkaline solution via substantial reduction of Co (III) to Co (II) and Ni (III) to Ni (II). The abundance of functional groups on MXene's surface makes them the most suitable carriers to immobilize the active analytes, further enhancing electrochemical biosensing efficacy. For example, $Ti_3C_2T_x$ hybrid nanosheets immobilized tetrahedral DNA structures were used to monitor mycotoxin using a gliotoxin aptamer with a sensing range between 5 pM and 10 pM and LOD of 5 pM (Wang et al., 2019). Also, Liu et al. (J. Liu et al., 2019) manufactured a novel electrochemical biosensor with dual functionality to immobilize the urease enzyme on MXenes surface chemistries by glutaraldehyde to detect both the urea and creatinine in humans. The biosensor exhibited a linear sensing range of 0–3 x 10^{-3} M with a LOD of nearly 0.02 × 10^{-3} and 10–400 × 10^{-6} M with a LOD of 1.2 × 10^{-6} M for creatinine.

In addition to this, numerous sensors based on MXene-enzyme immobilization have been developed to monitor a wide range of analytes, namely pesticides, metabolic by-products, micronutrients, as well as parameters based on 2D material for sensing miRNA, and gliotoxin electrochemically (Ansari and Malhotra, 2022; Khunger et al., 2021; Lei

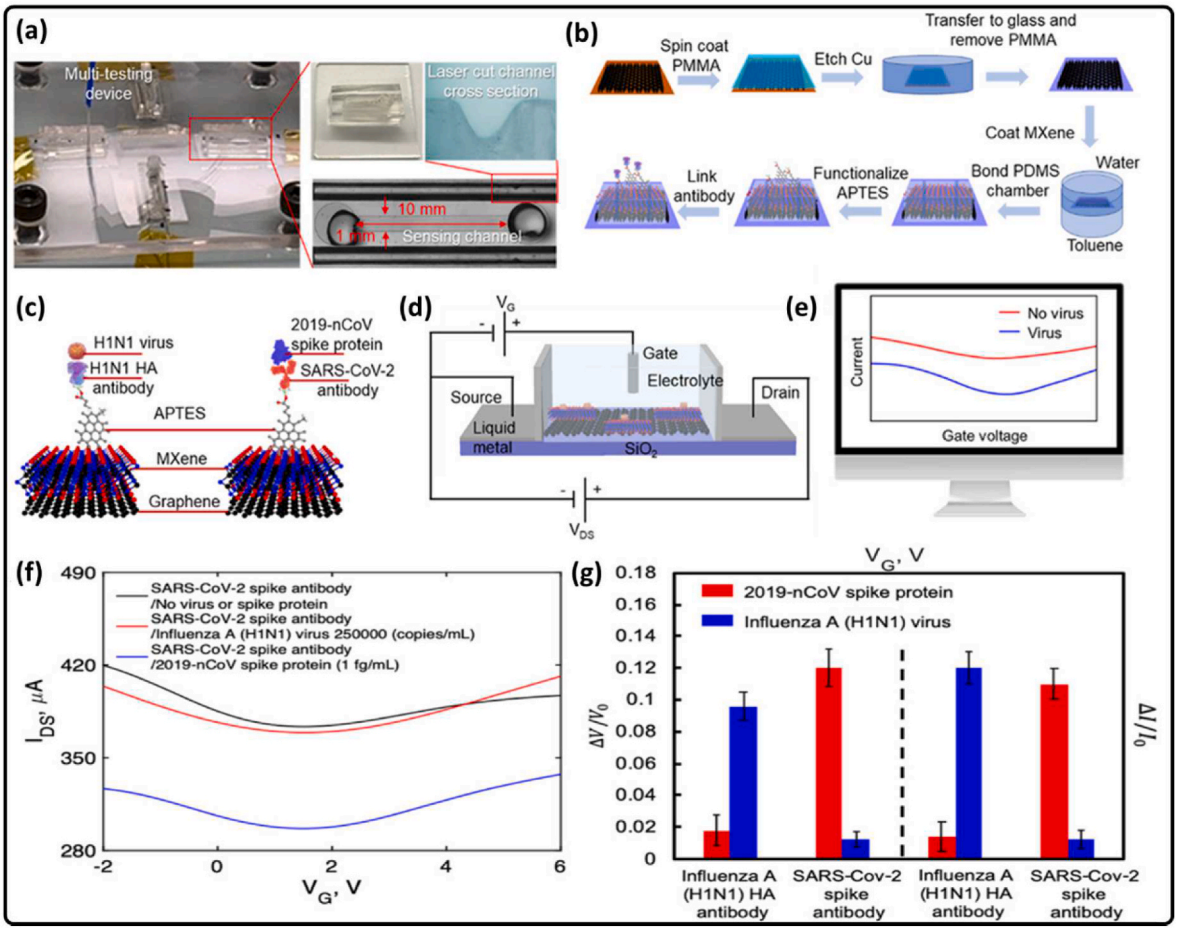

Fig. 11. (a) FET sensor based on Graphene-MXene hybrid (optical image) (b) Illustration of hybridization of graphene-MXene utilizing VSTM-deposition strategy. (c) Illustration of the related antigen-antibody-based monitoring process. Schematic illustration of (d) used FET circuit, (e) Changes in drain-source characteristics due to interaction with viruses, and (f) FET characteristics of SARS-CoV-2 spike antibody-immobilized biosensor. (g) Normalised drain-source and gate-voltage characteristic variation with STDs in overt binding assessment (Li et al., 2021).

et al., 2019; Novoselov et al., 2004). For instance, Zhao et al. (2022) developed a unique process of detecting microRNA-21 (miR-21) without a label. MXene-MoS_2 heterostructure also exhibited an enhanced catalytic hairpin assembly (CHA) signal strategy. The synergistic effect of MXene-MoS_2 and CHA demonstrated high detection performance to miR-21 by providing a hybrid with excellent conductivity, accelerating the electron transfer rate during the detection phenomenon. The sensor showed a low LOD of 26 fM and a wide sensing range of 100 fM to 100 nM.

Interestingly, biosensors with MXenes have appeared as potential devices for monitoring harmful viruses, particularly SARS coronavirus-2 (Y. Li et al., 2021; Unal et al., 2021). Li et al. (Y. Li et al., 2021) developed a Ti_2C MXene incorporating graphene hybrid field-effect transistor (FET) detector for monitoring severe viruses, such as SARS-COV-2 and influenza viruses, as depicted in Fig. 8. The biosensor was able to detect viruses with a sensing range of 25–250000 copies/mL^{-1} for H_1N_1, and 1–10 $pgmL^{-1}$ and LOD of 125 copies/mL^{-1} for recombinant spike protein 2019-nCoV and H_1N_1 virus, respectively, and 1 $FGmL^{-1}$ for recombinant 2019-to in the range of 50 ms. Apart from this, DNA-based MXene's-based chemical resistive biosensor is capable of sensing rapidly and selectively the SARS-CoV-2 nucleocapsid genes. The produced sensor had a substantial LOD of 105 copies/mL in sensing saliva while considerable selectivity against SARS-CoV-I and MERS (Fig. 11).

The exceptional sensing performance was ascribed to the diversified surface-terminating terminals of $Ti_3C_2T_x$ offering large number of binding sites for (3-aminopropyl) triethoxysilane (APTES) to hold target viruses. Moreover, the antigen-antibody sensing mechanism was explained in term of surface charge compensation during the binding event leading to variation in drain-source current–voltage response, which is recorded as sensing outcomes.

5.2. *Advancements in the MXene-based photo- and calorimetric-type biosensors*

Due to surface and quantum confinement effects, MXenes display strong photoluminescence. This attribute can measure biomolecules and execute cell imaging (Bai et al., 2022; Chen et al., 2018; Guan et al., 2019; Li et al., 2019; Liu et al., 2020; Liu et al., 2019; Mannoor et al., 2012; Xue et al., 2017; Xun et al., 2021) This can primarily be ascribed to the discrete energy levels present in the quantum dots based on different 2D materials, wherein excitations can mainly undergo radiative decay. Xue et al. (2017) performed multicolor RAW264.7 cells imaging using a hydrothermally produced biocompatible QDs sensor based on MXene having rich N-surface chemistries. As the vast majority of QDs occurred in the cytoplasm and were substantially lesser in levels at the nucleus, the prospect of QDs causing genetic modification was extremely low. Several reports have been signifying using QDs based on MXene to perform cellular imaging of the NIH 3T3 fibroblast cells and macrophage human cells.

Chen et al. (2018) described a biosensor with dual function based on $Ti_3C_2T_x$ QDs/Tris (bipyridine) ruthenium (II) chloride ($[Ru(DPP)_3]Cl_2$) nanocomposite to detect intercellular pH as well as to capture cellular imaging, in perspective to use as a viable biosensing system to fabricate

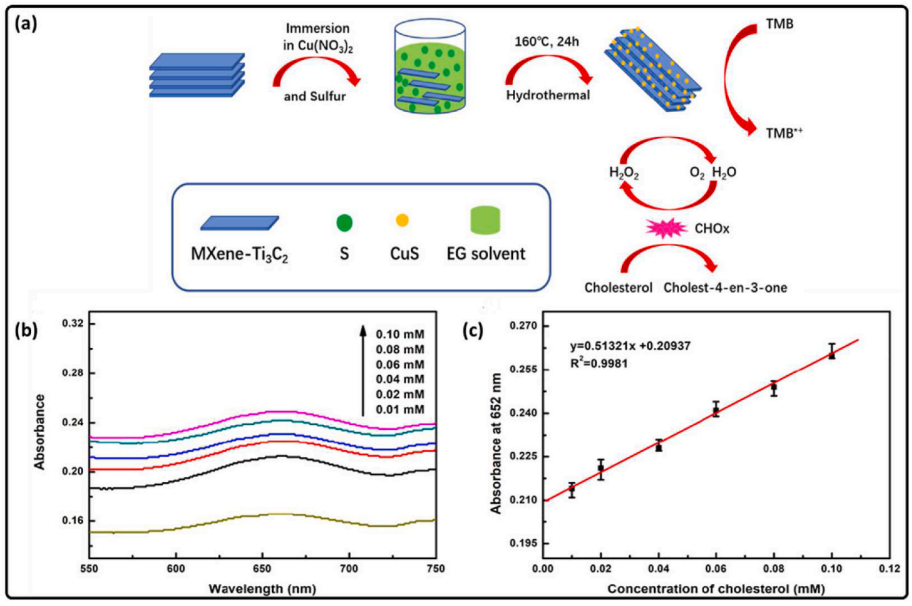

Fig. 12. (a) Preparation scheme of the fabricated MXene and CuS nanocomposites. (b) UV–Visible spectra comparison of MXene/CuS and TMB having the pH of 3.5 Hac-NaAC buffer at 37 °C (Y. Li et al., 2019).

fluorescent embedded wearable sensors. It was entirely based on the pH-reliant PL response of MXene-QD incorporating $[Ru(DPP)_3]Cl_2$ nanocomposite. The $[Ru(DPP)_3]Cl_2$ had been unresponsive to pH at 615 nm, whereas QDs have been extremely sensitive at 460 nm. Also, the correlation between PL and pH has been linear ranging between 5 and 9. Thus, it is evident that MXenes QDs can simultaneously perform two tasks, namely monitoring the pH and cell imaging. Furthermore, Liu et al. (2020) developed a radiometric sensor based on glutathione (GSH) and MXene-QD nanocomposite, which assisted in detecting UA with the naked eye. The inclusion of UA in the detecting mechanism, which also contains urate oxidase (uricase), o-phenylenediamine (OPD), and horseradish peroxidase (HRP), results in the production of hydrogen peroxide to oxidise OPDs. The peak for UV absorption of 425 nm for oxidized OPDs, and the peak for PL of 430 nm for the composite (GSH/MXene-QD) over-lapses, suggesting the transition of fluorescent resonance frequency takes place from GSH/MXENE-QD toward oxidized OPDs under the influence of UA. For UA, the sensor depicted a low LOD (125×10^{-9} M). Since the oxidized OPDs are yellow, the biosensor can also work as a calorimetric form. When the level of UA in the GSH-MXene QD solution is raised in daylight and exposed to UV light, the color transforms to yellow from transparent, revealing its calorimetric effectiveness.

Ample calorimetric biosensors based on MXene have been discussed in this study for detecting glucose/dextrose, glutathione (an antioxidant), carcinoembryonic antigens in body fluids, and cholesterol. Li et al. (Li et al., 2019) synthesized a calorimetric sensor from MXene/CuS nanocomposite with a peroxides-type reaction to monitor cholesterol, as illustrated in Fig. 12(a) When cholesterol oxidase reacts chemically with the cholesterol, it produces hydrogen peroxide. In addition, it causes CUS NPs to combine over the surface of MXene to form blue colored TMB^+ ions. As a result, the color of the solution progressively turns from transparent to blue as the content of cholesterol increases. Still, simultaneously the sensor showed a lower LOD of 1.9×10^{-6} M in Fig. 12(b).

Similarly, GSH was also measured through a calorimetric detector fabricated using MXene/NiFe nanoflake composite (Li et al., 2020). This has been observed that with increasing GSH contents, the color of the mixture changed from blue to transparent white due to the elimination of TMB ions. Also, the designed sensor behaved linearly with a detection range of 0.9–30 $\times 10^{-6}$ M and LOD of 84 $\times 10^{-9}$ M.

5.3. Advancements in electrochemiluminescence-type MXene-biosensors

Biosensors that operate in the electrochemiluminescence (ECL) state have widespread use in medical diagnostics. It is primarily due to three main reasons. Firstly, they are capable of reducing background noises. Secondly, they provide a wide detection range and finally, they possess high sensitivity. ECL-based sensors operate on an electro-generated chemiluminescence signal that experiences an exergonic chemical reaction to activate luminophores that emit light upon returning to initial operating conditions. ECL is an ideal approach for detecting biomaterials that govern intercellular communication, such as exosomes. It is a potential non-invasive diagnostic tool for detecting and tracking pathogens, including malignant tumor cells. For example, Zhang et al. (Zhang et al., 2019) described an exosome-based biosensor derived from a breast tumor cell line (MCF-7). Exosomes were initially grown on Au NP/poly (N-isopropyl acrylamide) and (AuNP/PNIPAM)-modified GCE, combining an aptamer with an amino-based functional batch. The nanoprobes based on MXene have been synthesized after MXene's electrostatic surface modification with different aptamer and PEI. The research findings indicated that the luminol solution's PL intensity was 5-fold higher for manufactured nanoprobe than the pure GCE, which supports MXene-based aptamer nanoelectrodes for exosome sensors. It had linear detection sensitivity of 500–5000000 particles/μL and LOD of about 125 particles/μL. In this study, MXenes nanosheets serve a dual function of catalyzing the ECL process of luminol and providing a larger surface area for loading a mass of Apt2, felicitating the exosomes capture.

Also, Fang et al. (2020) described MXene/tris (4,4′-dicarboxyl-2, 2′-bipyridine) ruthenium (II) ion ($Ru(dcbpy)_3^{2+}$) (an organic dye)/black phosphorus-based exosome QD sensor having LOD of about 37 particles/μL. Similarly, Wang et al. (Wang et al., 2022) detected DNA phosphorylated with polynucleotide kinase (PNK) using a $Ru–Ti_3C_2T_X$-AuNPs ECL sensor having 0.002–10 U mL^{-1} of linear sensing range and 0.0002 U mL^{-1} LOD. The improvement in sensing action was ascribed to the MXene providing magnification efforts and anchoring locations for auxiliary hybrid nano-devices in the ECL sensor. Furthermore, Fang et al. (2018) in another study utilized MXene/Ru $(dcbpy)_3$ to improve GCE to distinguish individual nucleotide variations in urine samples. It is expected to result in a genetic mutation based on severe illnesses in humans. The detection process is sensitive to the

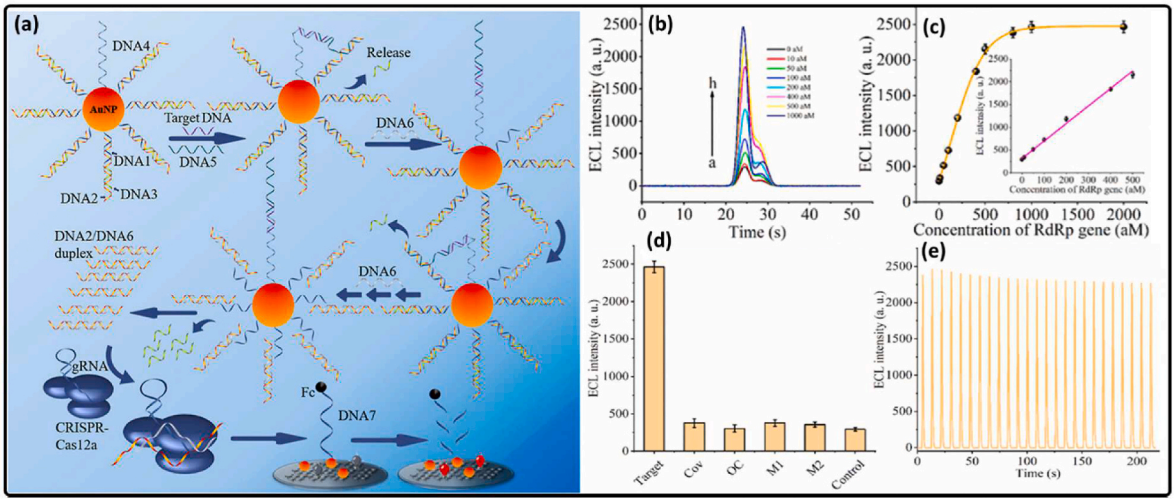

Fig. 13. (a) Schematic depiction of the 3D-DNA walker-CRISPR Cas 12a-based ECL biosensor for sensing SARS-COV-2 RdRp genes. (b) Time-dependent ECL spectra for different SARS-CoV-2 RdRp gene's concentration of 0 aM–1000 aM, and association of SARS-CoV-2 RdRp gene's concentration with ECL observations. (With inset: Dependence of the ECL intensity over the concentration of SARS-CoV-2 RdRp gene. (c) Selectivity studies of ECL biosensor (Zhang et al., 2022).

concentration level of an individual-nucleotide difference, which, when bonded to MXene, causes a reaction with Ru $(dcbpy)_3$. The ECL sensor possessed 3-fold high sensing action for mismatched individual nucleotides compared to completely matched individual nucleotides, with 1×10^{-9} M LOD. In contrast to ECL modules, QDs based on MXene have been observed as biosensors in the photoelectrochemical module.

To illustrate, Chen et al. (2018) employed MXene based QD sensor to detect glutathione photoelectrochemically having a LOD of nearly 9×10^{-9} M. Likewise, a 2D Ti_2C MXene-based PEC biosensor with superior efficiency was fabricated for selectivity and detection of sCD146. The exceptional physicochemical properties of 2D Ti_2C MXene decreased the re-joining of photogenerated holes or electrons and enhanced the sensing behavior of the biosensor. At optimal values, the sensor displayed a linear detection range (LDR) of (0.1–1000 pg/mL) with LOD (18 fg/mL) (Jiang et al., 2022).

Remarkably, Zhang et al. (Zhang et al., 2022) explored an ECL-based biosensor to detect the SARS-CoV-2 RdRp genes by integrating two different strategies, namely 3D-DNA walker and CRISPR-Cas12a trans-cleavage operation with PEI-Ru@Ti_3C_2@AuNPs nanocomposite (Fig. 13(a)-(c)). As a result, the sensor showed 12.8 mM of LOD for detecting the SARS-CoV-2 RdRp gene. Furthermore, due to the active CRISPR-Cas2a, which separates individual-stranded DNA, the sensor's sensitivity improves significantly, causing one end of the DNA to disassociate from the detector surface. Contrary, Yao et al. (2021) used an Au@Ti_3C_2@PEI-Ru$(dcbpy)_3^{2+}$ based hybrid nanocomposite ECL sensor to detect the SARS-CoV-2 RNA-dependent RNA polymerase (RdRp) gene with 1 fM-100 pM of linear detection range and 0.21 fM of LOD. The luminescent attributes of AuNPs linked with Ru$(dcbpy)_3^{2+}$DNA fixed on MXene surface contribute to superior sensitivity of the ECL biosensor. Further, the interconnectivity of PEI with Ru$(dcbpy)_3^{2+}$ through an amide bond improved the luminous efficacy of the hybrid. Moreover, the amplification method using a unipedal DNA walker improved the detection efficiency of ECL biosensor. It was further activated using SARS-CoV-2 RdRp, which leads to the excision of HP DNAs bound to model DNA–AgNCs. The combination of these two strategies leads to high-performance of ECL biosensors in detecting SARS-CoV-2 RdRp gene.

Further, to screen severe COVID-19 patients, Mi et al. (2021) explored the use of a tetrahedral DNA/aptamer cardiac troponin-I biosensor based on an in-situ hybridised chain reaction on an Au/Ti_3C_2-MXene substrate. The sensor depicted a LOD as 0.04 fM and a sensing range of 0.1 fM – 1 pM towards cTnl. The designed sensor demonstrates an innovative method of screening COVID-19 patients in portable cabin healthcare facilities. Since installing Electrocardiogram apparatus at every required site and at home is complicated, the biomarker assays in peripheral blood is more cost-effective and prompt way. Moreover, such miniature biosensors have the potential to contribute towards designing HOC module biosensors.

6. Progressing towards hospital-on-chip strategies: intelligent and sustainable approach

The energy-saving, compact, affordable, transportable, simple design, wearable, highly flexible, skin-embedded, transparent, multipurpose, ultralight, excellent biocompatibility and fast sensing systems have transformed the sensor's world dynamically, culminating on the internet of nano-things (IoNT). Such monitoring means can be linked to Bluetooth devices, internet networks and each other, allowing for a meaningful, intelligent assessment of various environmental stimuli. The robustness of these sensors is outstanding, and they can endure intense pressure and environmental variations easily. Due to the modest size of core elements, sensors in IoT may be positioned at every conceivable stimulation location, allowing for more efficient, reliable and accurate data collection and monitoring compared with conventional IoT systems. IoT-based next-phase sensors can wirelessly sense stimuli and transmit signals directly to the recording and analyzing devices. IoT sensors have great potential to transform existing public management methods consuming less time, labor, and vital resources (Chaudhary et al., 2022c, 2022e; Kim et al., 2015; Lin et al., 2020; Mannoor et al., 2012; Neampet et al., 2019; Qian et al., 2022; Scott et al., 2022; Shahzad et al., 2019; Sheth et al., 2022; Verma et al., 2022; Wu et al., 2019; Yao et al., 2020). For example, associating IoT sensing devices to COVID-19 diagnostics enables the production of a HOC system that can identify SARS-CoV-2, even in the most remote areas connected to modern healthcare centers.

Guanhua et al. (Xun et al., 2021) reported the fabrication of the most accessible and most scalable testing system for COVID-19 detection, which includes the rapid, entirely accurate and sensitive assay likely to battery-based portable powdered devices. Similarly, various relatable samples have been collected from the human body to diagnose several infectious diseases which deadly viruses and pathogens can cause. But all tears, saliva and body sweat can be collected in a non-inverse way. In contrast, saliva contains the variation of biomarkers naturally created from external substances, microorganisms, and salivary glands. Therefore, to identify and protect from all these point-of-care and lab-in-a-mouth based sensors are also utilized to monitor health,

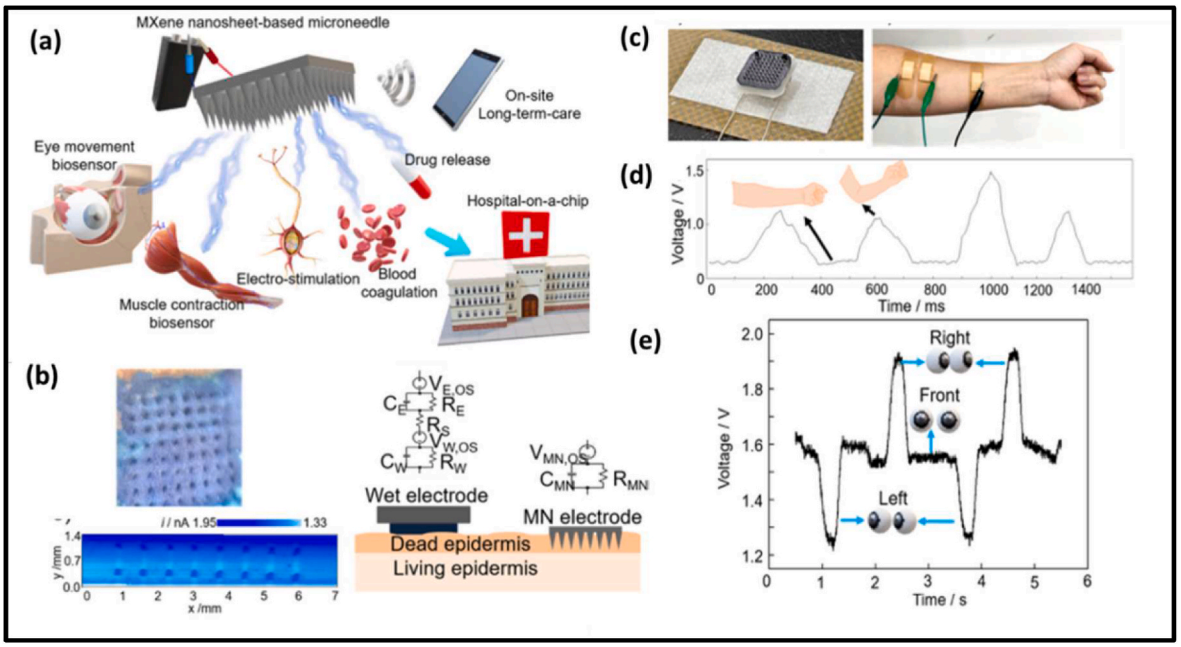

Fig. 14. Hospital-on-chip module: (a) Illustration using multifunctional MXene-based microneedles. (b) Schematic depiction of the bioimpedance model of the traditional microneedle and wet electrode module on the epidermis and optical micrographs of microneedle penetrated the skin. (c) Optical micrograph of the MXene-microneedle over bandage and wearable biosensor based on MXene over the arm. (d) Sensitivity of biosensor by voltage produced by bending the elbow. (e) Sensitivity of biosensors by voltage produced by the movement of the human eye (Yang et al., 2021).

infection, and pathogens status. Mannoor et al. (2012) produced saliva-based graphene wearable sensors, which help to detect the H-pylori results from the body to diagnose stomach and liver diseases. In these sensors, they applied the printing method to combine the single layer graphene with soluble water-based silk fibroin films and fixed it on tooth enamel. Whereas, through this method, electrode patterns are designed on silk-based graphene films. Later this sensor is moved onto the tooth's surface related to the root canal and other activities.

Kim et al. (2015) also reported that wearable sensors for detecting salivary uric acid, together with integrated and portable wireless devices, are utilized for the concentration of salivary uric acid. Lin et al. (2020) reported the soluble PVP microneedle therapeutic system encumbered with the Nb_2C-based MXene NS for photothermal ablation and implantation of superficial tumors in the 2nd NIR biological windows. According to the report, it was noticed that at 70 °C, tumor temperature increased under the irradiation source of 1064 nm, which further possesses enough bearable conditions for the photonics-based tumor ablation. The same group in another study reported the Nb_2C MXene by utilizing the 1st and 2nd NIR biological window for the photothermal tumor detection, in which the sample yields the conversion efficiency of 36.4 and 45.65% for both NIR-I and NIR-II windows, respectively. Later, Yang et al. (2021) successfully developed a HOC device using an MXene nanosheet-based multipurpose microneedle, as shown in Fig. 14((a)-(e)).

The biosensor built with a single chip has enhanced human diagnostics and remedial therapeutics like a micro-hospital. Through puncturing the dead skin, MXene-microneedles aid in medication delivery. Additionally, it can identify even a minor potential disparity inside the body brought on by arm muscle and eye movements. Furthermore, the biosensor is multifunctional, much like a hospital unit. Thus, incorporating IoT sensors has enormous potential for building e-healthcare facilities that are intelligent, adaptable, and interoperation. Biosensor connected with IoT using MXene is uniquely addressed and identifiable by the internet worldwide and at any time to detect, monitor, store, evaluate, and reply to the signal. Also, they can send information immediately to any location in the world that is linked to the internet, designed to simplify setup, process, and administration tasks. These intelligent sensors based on IoT can be used in intelligent alarms on little modifications in specific stimuli and to prevent and manage serious global issues. IoT sensors, for example, can be developed utilizing thermally stable MXenes to observe volcanoes erupting, reducing enormous resource and human life loss. Moreover, using the idea of nano-triboelectric attributes of MXenes or their interface with several more triboelectric resources, they can function on a self-sustaining model that does not require an external power source.

Computational and analytical technologies, including Al, Dl, ML and data analytics, are progressing rapidly with applications that extend beyond information technology (IT) to materials and sensor design. They offer incredible potential as an enhanced forecasting and accurate sensing operating tool. Before enduring experimental analyses, technologies such as AI and ML are used to forecast the performance, limitations theoretically, and alternative remedies related to the functioning of the particular sensor, resulting in time, expenditure, materials, contamination, and human resources savings. For example, while designing breath analyzing sensors, AI and ML can operate together to gather different information from human exhaled breath and evaluate large datasets of digitized biomarkers using the DL method to develop prognostic evaluations of physiological details and facts. As a result, it can improve the assessment of effective medications, specific drug responses, and the accurate drug dose for each patient. Likewise, previous stimulus responses can enhance sensing device performance. A distinctive aspect is that relevant data can be accessed and measured with an intelligent computing device or cellular mobile device. However, implementing AI within future sensors can segregate operational data from the massive data obtained through regular monitoring of particular stimuli. Therefore, researchers need fast progress of more advanced algorithms for pre-processing and elucidating the practical information to produce huge-data-based estimations, such as early diagnostics of chronic ailments or early recognition of leakage, particularly gases, which can benefit humanity to a great extent.

7. Challenges, potential solutions, and prospects

Most viable, efficient, widespread, and sensitive methodologies for

designing various sensors depend on the availability of inorganic nanomaterials, mainly metal oxides. Using inorganic elements, on the other hand, introduces obstacles in a particular family of sensors. For example, metal oxide-based chemical detectors need high-temperature processes, which raise their cost, energy usage, and reduces lifetime. However, the environmental contamination caused by the incorporation of hazardous compounds, sulphur poisoning, poor biocompatibility, limited flexibility, toxicity, and restricted sensitivity is significant downsides of these sensors. It reduces the feasibility of metal oxides for machine processing and easy integration into wearable future-generation sensing devices.

The emergence of MXenes and other 2D nanomaterials, like graphene, have transformed the world of sensors dynamically, which will benefit humanity eventually. To demonstrate, wearable biosensors embedded with transparent skins for non-invaded and rapid monitoring of human well-being via exhaled breath are technological breakthroughs. Additionally, sensing, and scavenging virus-laden aerosols and other air pollutants could be a potential strategy for combating infectious illnesses and achieving a sustainable environment. Particularly in this period of the COVID-19 pandemic, MXenes can aid in designing diagnostics and therapeutics. Sensors using MXenes can achieve remarkable and tunable physicochemical properties, such as large specific area, hydrophilicity, adjustable electronic as well as optical bands, improved dispersibility, enhanced surface terminal functionalities, more flexibility and optimal porosity.

Nonetheless, despite the enormous diversity of MXene stoichiometry, phases, and architecture, many researchers have focused on analyzing the sensing outcome of $Ti_3C_2T_x$. It increases a significant gap among theoretical anticipations, in-laboratory technology, applicability, and commercial usability. Machine processing, DL, and ab-initio computations are practical tools for researchers investigating exact stoichiometry, interactions, and architecture of MXenes with next-generation sensing insights. For example, simulation was initially used to predict the prospects of MXenes for sensing purposes. However, simultaneous computation and experimental analysis of MXene-based biosensors are required for long-term fast development.

Further, for the mass production of MXenes-based sensors, scalable but low-temperature fabrication of MXenes has become a key benefit. Furthermore, the effective production of MXene free-standing films has depicted their practical incorporation in flexible, wearable, and lightweight mobile sensors. Sensor designing methodologies that are diverse, scalable, environmentally sustainable, affordable, repeatable, and power-saving are critical to merging technology for producing MXene-based sensors for future generations.

Although MXenes have demonstrated significant potential in designing physicochemical biosensors with outcomes equivalent to or higher than previously developed sensing materials, they still face several fundamental obstacles in terms of commercial opportunities. However, other solutions, such as strategically designed exclusive protocols, have been proposed to resolve these limitations. Consequently, MXenes-based biosensors are significantly concerned with establishing secure techniques, energy savers, machine-processing, affordable and increased productivity.

7.1. Improvements in fabrication

The present MXene developing processes are influenced by severe corrosive chemical reactions, which negatively impact the ecosystem. Even the more improved, advanced and highly developed in-situ chemical synthesising techniques contaminate the ecology to some degree. To exemplify, fluorinated chemical manufacturing procedures produce far more fluorine compounds on the surface of MXene, which can be harmful to gas and VOC sensing action. It prompted the exploration of alternate manufacturing technologies, such as chemical vapor deposition (CVD) or salt-templating methods. However, the applicability of salt-template techniques is limited since the structure of MXenes depends on the crystalline structure and crystal geometries of specific precursors.

On the other hand, CVD has been a more feasible synthesising process to manufacture a few layers MXene, such as M_2X-MXene. However, synthesising higher order MXene using CVD is challenging due to their metamorphism structure and multifarious stoichiometry. Also, CVD, MBE and other mechanical alternative techniques produce a limited yield of terminated 2D materials. Another stumbling block is the practical storage and post-processing of MXene, as they are unstable in humid and oxygen-rich conditions. Even though there are other methods for storing and post-processing them, they are still more complicated, expensive, laborious, and time-consuming. Therefore, more improved, and advanced synthesis processes can be developed to achieve a high yield of MXenes with suitable surface characteristics for focused sensing applications.

7.2. Improvements through hybridization

Considering the issues associated with cutting-edge MXene-based sensor technology, the most favourable approach is to design secondary nanomaterials hybrids. For instance, macromolecules can provide significant flexibility in fabricating wearable sensing devices. However, scalable fabrication of such hybrids demands optimal precursor concentration. This is highly challenging to achieve, which limits their commercial viability. For example, the flexibility achieved by incorporating macromolecules occurs at the expense of MXenes' electrical conductivity.

Further, during hybrid machine processing, the interaction between MXene's mechanical strength and the flexibility of macromolecules arises. Also, if the concentration of a precursor is higher than a specific limit, it would deplete the quality of another. At the same time, a greater concentration of one precursor can degrade the effectiveness of another. For instance, adding polymers in MXene layers raises the interlayer spacing, causing a specific strain that disrupts MXene's conducting network. By contrast, the increased MXenes concentration causes the metal conductivity to lose its semiconducting properties.

Consequently, a simultaneous balance must occur between the precursor concentration rate, processing, and operational conditions. It includes diverse tribological analyses to evaluate the concentration of a threshold precursor in the hybrid with predicted attributes. These findings indicate the trade-offs between the concentration of the precursor and the processing elements of hybrids.

7.3. Improvements in sensing characteristics

Sensors based on non-oxide materials undergo atmospheric oxidation and degradation due to humidification. Thereby, the lifespan of the non-oxide-based sensor declines substantially. Besides this, MXenes are also susceptible to surface oxidation and deterioration, particularly when stored at ambient temperature conditions. Consequently, it degrades the sensor's efficacy and reduces its operating life. Hence, this hindrance must be handled before developing a sensor for a specific application. Several distinct approaches have been proposed to increase surface stability, such as using secondary nanomaterials/coatings. However, reproducing the sensor's reproducibility and repeatability over time remains challenging.

Furthermore, pristine MXenes are highly sensitive to numerous stimuli, such as toxic gases, fumes, humidity, and biomes, culminating in an identical deceitful response. In contrast, it aids in the development of multipurpose sensors capable of sensing distinct stimuli at the same time. In contrast, it increases cross-sensitivity in sensors which is undesirable for their design as it might result in inaccurate stimuli identification and quantification. For example, monitoring biomarkers in human breath through non-invasive biosensors is strongly inferred by the moisture in exhaled breath produced by biological metabolism. Subsequently, a sensor must have a high anti-interference potential for

unwanted stimuli to ensure its durability and precision. It can be attained by categorising the detected signals per their character and origin using the most suitable electronically integrated circuits and systems based on AI. Numerous advanced techniques, including AI, artificial neural networks (ANN), pattern recognition, and data evaluating tools, are critical in developing favourable intelligent modules that can address the cross-sensitivity bottleneck.

Next-generation wearable biosensors coupled to the body need constant data processing, which is critical for monitoring environmental stimuli modifications. MXenes can promptly respond to stimuli changes and return to their original form between a few seconds and hundreds of seconds. However, they exhibit a deliberative reaction and response to various stimuli, restricting their realistic prospects. This is owing to the strong binding forces of sophisticated 2D surfaces in the direction of particular analytes or biomarkers. Furthermore, it causes the sensor to take a prolonged time to reform to its initial position, extending the restoration time to hundreds of seconds from a few. Still, the short response and recovery time, particularly in milliseconds, of revolutionary sensors is not only indispensable but also highly required. All these challenges can be resolved by investigating various sensory device architects, such as using interdigitated probes rather than conventional parallel conducting electrodes, hybrid/nanocomposite secondary materials, surface alterations, and incorporating rapid data collecting techniques.

7.4. Exploring theoretical predictions

Although rapid progress and significant simulative projections of MXenes with distinct stoichiometry, architectures, and phases, relatively few have been validated experimentally for sensing functions, indicating a huge gap between theoretical sensing calculations and their actual implementations. So far, for instance, a small number of 2D material phases have been developed experimentally and on a couple of substrates. In contrast, researchers have focused far less on nitride based MXenes than MXenes based on carbide. Despite the tremendous possibilities of these microstructure and phase modifications, as well as stoichiometric and layer-based alterations in MXenes, relatively few have been tuned for sensing applications. Moreover, researchers have done little research on hybrid nanocomposites, although ample materials are available. Therefore, it is noticeable that MXenes have been immensely unexplored unconfirmed possibilities based on morphological and chemical composition that may be used to accomplish progressive and innovative sensing needs. To illustrate this point, selectivity to sense nitro-oxide can be attained through optimal hydrogenation and in MXenes through careful transition metal selection. Hence, by selecting the most suitable chemical and structural compositions, scalable production, and superior machine processing, the difference between the theoretical evaluations, experimental technologies, applied analysis, and viable advancement of MXenes may be bridged.

7.5. Cutting-edge sustainable prospects of MXenes

Distinct biosensors, which may be functioning physically, chemically, and biologically, are revolutionising nearly every industry that requires real-time assessments, rationalized decision-making methods, and intelligent workability, thanks to the integration with techniques like AI and IoT. Moreover, the world is becoming increasingly intelligent and sophisticated based on smart communities, astute farming, innovative technology, and intelligent medical services. Over the next ten or more years, 150 billion network-based monitoring sensors coupled with IoTs are expected to be implemented globally. The sustainable development of sensing devices relies on several factors that depend on the particular component. These factors include energy efficiency, eco-friendliness, recyclability, greener manufacturing, biocompatibility, and biodegradability. For example, substrates, electrical circuitry components, such as PCB boards and cables, probes, and detecting materials should be ecological and user-friendly. Also, they must be fabricated using greener methods, such as bioinspired/biodiverse substances, or the outcome must be environmentally beneficial(Batra et al., 2022; Chaudhary, 2022; Chaudhary et al., 2022a). For example, Verma et al. (Abdolhosseinzadeh et al., 2020) developed a pristine MXene-based $Ti_3C_2T_x$ liquid ink for large-scale printing applications, with possible applications in 3D and 4D printed sensing device manufacturing.

Interestingly, the ink was produced using the "treasure from trash" concept, which included making ink from unetched chemical precursors and several layer MXenes residues generally left after delamination—producing ink by reprocessing the refused substance into worthy material for screen printing. It reveals that the unused recyclable MXene can be used for substrate printing for workable and scalable production of 5^{th} generation wearable intelligent sensors. Furthermore, applying such large-scale sensors must not generate solid waste issues. These materials must be reusable or biodegradable, and they must be conveniently discarded after their intended usage. For instance, Geravand et al. (Abbasi Geravand et al., 2021) developed a novel biodegradable nano-filtration membrane using a hybrid nanocomposite fabricated from polycaprolactone (PLC) and $Ti_3C_2(OH)_2$ hydrophilic MXene sheets for the treatment of dyed aqueous solutions. Also, Zhang et al. (W. Zhang et al., 2022) revealed an intriguing biodegradable multipurpose pressure sensor developed using cross-attached collagen fibres (CCFs) with MXene aerogel exhibiting a great sensitivity response of 61.99 kPa^{-1} within a short time of 0.30s, speedy recovery within few milliseconds of 0.15s, high thermal steadiness, and small LDL (0.4 kPa).

Moreover, immersing the aerogel in an alkaline medium destroys it in forty days. The degradation rate is attributed to using whole natural fibres in aerosol production. Energy sustainability has been accomplished in sensing devices through self-operating aspects or ambient temperature functioning. It is clear from the earlier discussions that MXene-based sensors can sense stimuli at ambient temperature, preserving energy for dynamic performance. Furthermore, the incorporation of triboelectric nanogenerators in MXenes has already initiated the transformation of wearable electronic devices with sensor integration (Lei et al., 2020; S. Li et al., 2020; Tan et al., 2020; Xin et al., 2020). In addition to this, based on the application area, the complete unit of smart sensing sets can be operated on green energy resources, such as triboelectricity, wind power energy, hydrothermal energy, tidal wave energy, and sun-powered energy. For instance, farming based on intelligent sensors can be powered by sustainable solar energy via rapidly recharging solar panels (Sonu and Chaudhary, 2022). Depending on the application, motion detectors deployed in submarines or ship bottom decks can be designed to work on ocean-based sustainable energy. MXenes are employed in developing the 5^{th} generation of nanogenerator-based triboelectric generators that can be coupled with MXene sensing devices to provide autonomous operation. For example, an intelligent wristwatch linked with a particular oxygen detector can be powered by the back-and-forth motion of the hand using triboelectric principles. Thus, sensors based on MXene have great potential to assist in achieving various sustainable development goals (SDGs).

8. Conclusive outlook and viewpoint

This article discusses the rise of the paradigm of intelligent biosensors, generally focusing on the lab-on-a-chip module progressing towards the hospital-on-chip model. These biosensor modules possess diversified applications such as clinical devices, hospital needs, and personalized healthcare monitoring, especially in the COVID-19 scenarios, to protect human lives. The practical applications of these biosensors are usually demanded in the medical world, which is tranquil in its beginning by utilizing various kinds of nanomaterials, such as 2D materials, transition metals dichalcogenides, and organic and inorganic materials. Among all, MXene-based biosensors are the most up-and-coming class owing to their remarkable properties and applications, which are necessary for devising future generation biosensors with

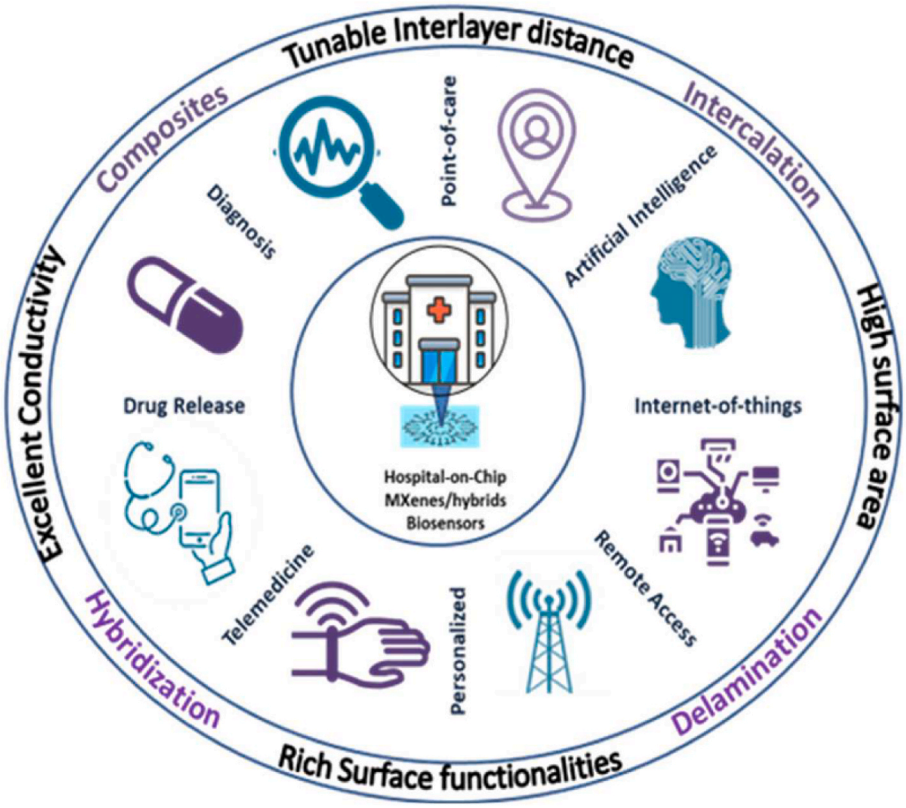

Fig. 15. Prospects of MXenes based 5th generation biosensor with the integration of modern-age technologies.

intelligent and on-site modules.

Additionally, the advantages of MXene-based intelligent biosensors depicts mobility, compactness, wearability, smartness, intelligence, innovative 3D and 4D printable features, multifunctionality, point-of-action, single-chip function, remote monitoring, self-driven, selectivity with the inclusion of IoNTs, AI, ML, cloud computing, and 5G technologies are all 5th generation aspects (Fig. 15). These innovative prospects and potential alternatives can only be realized through the collaborative endeavors of material scholars, designers, data analysts, informatics, environmental activists, health care workers, legislators, and industries to commercialize MXenes as advanced sensing materials. Therefore, MXenes are expected to increase and develop in all real-world areas to construct 5th generation smart and intelligent sensors with sustainable and scalable characteristics. In addition, these kinds of integrated intelligent biosensors are welcoming the ways toward the electronic, portable, and cost-effective HOC based diagnosis platforms that could be easily applicable both inside and outside the hospitals, houses, clinics and other medical premises, especially in remote areas.

However, there are still some restrictions in this research in which the integration of all the applied arts in only a single frame and their connection with the worldwide applications should be overwhelmed. Nevertheless, these HOC module-based biosensors are the future of modern-age wearable, portable, compact, energy-efficient, and cost-effective healthcare devices to reach even the world's remotest area. Furthermore, it will help attain the sustainable development goals of human healthcare and well-being by accessing every individual with healthcare facilities. Hence, hospital-in-chip biosensors possess the potential to transform the current healthcare system into a miniature solution to control future mortalities and severities due to fatal and infectious diseases.

Declaration of competing interest

The authors declare that they have no known competing financial interests or personal relationships that could have appeared to influence the work reported in this paper.

Data availability

No data was used for the research described in the article.

Acknowledgements

All authors acknowledge their respective institutions/universities for overall support. VC also acknowldeges GOING GLOBAL PARTNERSHIPS EXPLORATORY GRANT (UNIQUE APPLICATION ID: 877799913) awarded by BRITISH COUNCIL of project entitled "ENHANCING COMMERCIAL ACUMEN AND ORGANISATIONAL CAPABILITY IN BUISNESS (ECOBUSS)". MK acknowledges Sunway University's International Research Network Grant Scheme (STR-IRNGS-SET-GAMRG-01-2022) for this work. YKM thanks the funding from Interreg Deutschland-Denmark with money from the European Regional Development Fund, project number 096-1.1-18 (Access and Acceleration) and also to Mads Clausen Institute, SDU Denmark.

References

Abbasi Geravand, M.H., Saljoughi, E., Mousavi, S.M., Kiani, S., 2021. Biodegradable polycaprolactone/MXene nanocomposite nanofiltration membranes for the treatment of dye solutions. J. Taiwan Inst. Chem. Eng. 128, 124–139. https://doi.org/10.1016/j.jtice.2021.08.048.

Abdolhosseinzadeh, S., Schneider, R., Verma, A., Heier, J., Nüesch, F., Zhang, C.J., 2020. Turning trash into treasure: additive free MXene sediment inks for screen-printed micro-supercapacitors. Adv. Mater. 32, e2000716 https://doi.org/10.1002/adma.202000716.

Aghamohammadi, H., Amousa, N., Eslami-Farsani, R., 2021. Recent advances in developing the MXene/polymer nanocomposites with multiple properties: a review study. Synth. Met. 273, 116695 https://doi.org/10.1016/j.synthmet.2020.116695.

Ahmed, B., Ghazaly, A. El, Rosen, J., 2020. i -MXenes for energy storage and catalysis. Adv. Funct. Mater. 30, 2000894 https://doi.org/10.1002/adfm.202000894.

Alwarappan, S., Nesakumar, N., Sun, D., Hu, T.Y., Li, C.Z., 2022. 2D metal carbides and nitrides (MXenes) for sensors and biosensors. Biosensors and Bioelectronics 205, 113943. https://doi.org/10.1016/j.bios.2021.113943.

Ansari, A.A., Malhotra, B.D., 2022. Current progress in organic–inorganic hetero-nano-interfaces based electrochemical biosensors for healthcare monitoring. Coord. Chem. Rev. 452, 214282 https://doi.org/10.1016/j.ccr.2021.214282.

Bai, Y., He, Y., Wang, M., Song, G., 2022. Microwave-assisted synthesis of nitrogen, phosphorus-doped Ti3C2 MXene quantum dots for colorimetric/fluorometric dual-modal nitrite assay with a portable smartphone platform. Sens. Actuators, B 357, 131410. https://doi.org/10.1016/j.snb.2022.131410.

Batra, V., Kaur, I., Pathania, D., Sonu, Chaudhary, V., 2022. Efficient dye degradation strategies using green synthesized ZnO-based nanoplatforms: A review. Applied Surface Science Advances 11, 100314. https://doi.org/10.1016/j.apsadv.2022.100314.

Berdiyorov, G.R., 2016. Optical properties of functionalized Ti 3 C 2 T 2 (T = F, O, OH) MXene: first-principles calculations. AIP Adv. 6, 055105 https://doi.org/10.1063/1.4948799.

Besher, K.M., Subah, Z., Ali, M.Z., 2021. IoT sensor initiated healthcare data security. IEEE Sensor. J. 21, 11977–11982. https://doi.org/10.1109/JSEN.2020.3013634.

Borysiuk, V.N., Mochalin, V.N., Gogotsi, Y., 2015. Molecular dynamic study of the mechanical properties of two-dimensional titanium carbides Ti n +1 C n (MXenes). Nanotechnology 26, 265705. https://doi.org/10.1088/0957-4484/26/26/265705.

Chae, Y., Kim, S.J., Cho, S.-Y., Choi, J., Maleski, K., Lee, B.-J., Jung, H.-T., Gogotsi, Y., Lee, Y., Ahn, C.W., 2019. An investigation into the factors governing the oxidation of two-dimensional Ti 3 C 2 MXene. Nanoscale 11, 8387–8393. https://doi.org/10.1039/C9NR00084D.

Chakraborty, P., Das, T., Nafday, D., Saha-Dasgupta, T., 2018. Manipulating the Mechanical Properties of Ti2C MXene: Effect of Substitutional Doping, 040008. https://doi.org/10.1063/1.5050748.

Chang, J., Yu, L., Li, H., Li, F., 2022. Dye sensitized Ti3C2 MXene-based highly sensitive homogeneous photoelectrochemical sensing of phosphate through decomposition of methylene blue-encapsulated zeolitic imidazolate framework-90. Sens. Actuators, B 352, 131021. https://doi.org/10.1016/j.snb.2021.131021.

Chaudhary, V., 2022. Charge carrier dynamics of electrochemically synthesized poly (aniline Co-pyrrole) nanospheres based sulfur dioxide chemiresistor. Polym. Technol. Mater. 61, 107–115. https://doi.org/10.1080/25740881.2021.1959932.

Chaudhary, V., 2021a. One-dimensional variable range charge carrier hopping in polyaniline–tungsten oxide nanocomposite-based hydrazine chemiresistor. Appl. Phys. 127, 536. https://doi.org/10.1007/s00339-021-04690-8.

Chaudhary, V., 2021b. High performance X-band electromagnetic shields based on methyl-orange assisted polyaniline-silver core-shell nanocomposites. Polym. Technol. Mater. 60, 1–10. https://doi.org/10.1080/25740881.2021.1912095.

Chaudhary, V., 2022. Prospects of green nanotechnology for efficient management of neurodegenerative diseases. Frontiers in Nanotechnology. https://doi.org/10.3389/fnano.2022.1055708.

Chaudhary, V., Ashraf, N., Khalid, M., Walvekar, R., Yang, Y., Kaushik, A., Mishra, Y.K., 2022a. Emergence of MXene-polymer hybrid nanocomposites as high-performance next-generation chemiresistors for efficient air quality monitoring. Adv. Funct. Mater., 2112913 https://doi.org/10.1002/adfm.202112913.

Chaudhary, V., Bhadola, P., Kaushik, A., Khalid, M., Furukawa, H., Khosla, A., 2022b. Assessing temporal correlation in environmental risk factors to design efficient area-specific COVID-19 regulations: Delhi based case study. Sci. Rep. 12, 12949 https://doi.org/10.1038/s41598-022-16781-4.

Chaudhary, V., Chavali, M., 2021. Novel methyl-orange assisted core-shell polyaniline-silver nanosheets for highly sensitive ammonia chemiresistors. J. Appl. Polym. Sci. 138, 51288 https://doi.org/10.1002/app.51288.

Chaudhary, V., Gautam, A., Mishra, Y.K., Kaushik, A., 2021a. Emerging MXene–polymer hybrid nanocomposites for high-performance ammonia sensing and monitoring. Nanomaterials 11, 2496. https://doi.org/10.3390/nano11102496.

Chaudhary, V., Gautam, A., Silotia, P., Malik, S., Hansen, R.O., Khalid, M., Khosla, A., Kaushik, A., Mishra, Y.K., 2022. Internet-of-nano-things (IoNT) driven intelligent face masks to combat airborne health hazard. Materials Today. https://doi.org/10.1016/j.mattod.2022.08.019.

Chaudhary, V., Kaur, A., 2015. Enhanced room temperature sulfur dioxide sensing behaviour of in situ polymerized polyaniline–tungsten oxide nanocomposite possessing honeycomb morphology. RSC Adv. 5, 73535–73544. https://doi.org/10.1039/C5RA08275G.

Chaudhary, V., Kaushik, A., Furukawa, H., Khosla, A., 2022c. Review—towards 5th generation AI and IoT driven sustainable intelligent sensors based on 2D MXenes and borophene. ECS Sensors Plus 1, 013601. https://doi.org/10.1149/2754-2726/ac5ac6.

Chaudhary, V., Mostafavi, E., Kaushik, A., 2022d. De-coding Ag as an efficient antimicrobial nano-system for controlling cellular/biological functions. Matter 5, 1995–1998. https://doi.org/10.1016/j.matt.2022.06.024.

Chaudhary, V., Royal, A., Chavali, M., Yadav, S.K., 2021b. Advancements in research and development to combat COVID-19 using nanotechnology. Nanotechnol. Environ. Eng. 6, 8. https://doi.org/10.1007/s41204-021-00102-7.

Chaudhary, V., Sharma, A., Bhadola, P., Kaushik, A., 2022e. Advancements in MXenes, pp. 301–324. https://doi.org/10.1007/978-3-031-05006-0_12.

Chaudhary, V., Singh, H., Kaur, A., 2017. Effect of charge carrier transport on sulfur dioxide monitoring performance of highly porous polyaniline nanofibres. Polym. Int. 66, 699–704. https://doi.org/10.1002/pi.5311.

Chen, X., Sun, X., Xu, W., Pan, G., Zhou, D., Zhu, J., Wang, H., Bai, X., Dong, B., Song, H., 2018. Ratiometric photoluminescence sensing based on Ti 3 C 2 MXene quantum dots as an intracellular pH sensor. Nanoscale 10, 1111–1118. https://doi.org/10.1039/C7NR06958H.

Chen, Z., Wang, Yikun, Han, J., Wang, T., Leng, Y., Wang, Yanmin, Li, T., Han, Y., 2020. Preparation of polyaniline onto dl -tartaric acid assembled MXene surface as an electrode material for supercapacitors. ACS Appl. Energy Mater. 3, 9326–9336. https://doi.org/10.1021/acsaem.0c01662.

Cherusseri, J., Savio, C.M., Khalid, M., Chaudhary, V., Numan, A., Varma, S.J., Menon, A., Kaushik, A., 2022. SARS-CoV-2-on-Chip for Long COVID Management 12 (10), 890. https://doi.org/10.3390/bios12100890.

Choi, J.R., 2020. Development of point-of-care biosensors for COVID-19. Front. Chem. 8 https://doi.org/10.3389/fchem.2020.00517.

Clark, L.C., Lyons, C., 2006. Electrode systems for continuous monitoring in cardiovascular surgery. Ann. N. Y. Acad. Sci. 102, 29–45. https://doi.org/10.1111/j.1749-6632.1962.tb13623.x.

Dhall, S., Mehta, B.R., Tyagi, A.K., Sood, K., 2021. A review on environmental gas sensors: materials and technologies. Sensors Int 2, 100116. https://doi.org/10.1016/j.sintl.2021.100116.

Dillon, A.D., Ghidiu, M.J., Krick, A.L., Griggs, J., May, S.J., Gogotsi, Y., Barsoum, M.W., Fafarman, A.T., 2016. Highly conductive optical quality solution-processed films of 2D titanium carbide. Adv. Funct. Mater. 26, 4162–4168. https://doi.org/10.1002/adfm.201600357.

Du, C.-F., Zhao, X., Wang, Z., Yu, H., Ye, Q., 2021. Recent advanced on the MXene–organic hybrids: design, synthesis, and their applications. Nanomaterials 11, 166. https://doi.org/10.3390/nano11010166.

Du, J.-F., Chen, J.-S., Liu, X.-P., Mao, C.-J., Jin, B.-K., 2022. Coupled electrochemiluminescent and resonance energy transfer determination of microRNA-141 using functionalized Mxene composite. Microchim. Acta 189, 264. https://doi.org/10.1007/s00604-022-05359-6.

Dwivedi, N., Dhand, C., Kumar, P., Srivastava, A.K., 2021. Emergent 2D materials for combating infectious diseases: the potential of MXenes and MXene–graphene composites to fight against pandemics. Mater. Adv. 2, 2892–2905. https://doi.org/10.1039/D1MA00003A.

Fang, D., Zhao, D., Zhang, S., Huang, Y., Dai, H., Lin, Y., 2020. Black phosphorus quantum dots functionalized MXenes as the enhanced dual-mode probe for exosomes sensing. Sens. Actuators, B 305, 127544. https://doi.org/10.1016/j.snb.2019.127544.

Fang, Y., Yang, X., Chen, T., Xu, G., Liu, M., Liu, J., Xu, Y., 2018. Two-dimensional titanium carbide (MXene)-based solid-state electrochemiluminescent sensor for label-free single-nucleotide mismatch discrimination in human urine. Sens. Actuators, B 263, 400–407. https://doi.org/10.1016/j.snb.2018.02.102.

Gautam, A., 2022. Towards Modern-Age Advanced Sensors for the Management of Neurodegenerative Disorders: Current Status, Challenges and Prospects. ECS Sensor Plus 1, 042401. https://doi.org/10.1149/2754-2726/ac973e.

Ghosh, S., Sachdeva, B., Sachdeva, P., Chaudhary, V., Mohana Rani, G., Sinha, J.K., 2022. Graphene quantum dots as a potential diagnostic and therapeutic tool for the management of Alzheimer's disease. Carbon Letters 32, 1381–1394. https://doi.org/10.1007/s42823-022-00397-9.

Gogotsi, Y., 2015. Chemical vapour deposition: transition metal carbides go 2D. Nat. Mater. https://doi.org/10.1038/nmat4386.

Gorton, L., Lindgren, A., Larsson, T., Munteanu, F.D., Ruzgas, T., Gazaryan, I., 1999. Direct electron transfer between heme-containing enzymes and electrodes as basis for third generation biosensors. Anal. Chim. Acta 400, 91–108. https://doi.org/10.1016/S0003-2670(99)00610-8.

Guan, Q., Ma, J., Yang, W., Zhang, R., Zhang, X., Dong, X., Fan, Y., Cai, L., Cao, Y., Zhang, Y., Li, N., Xu, Q., 2019. Highly fluorescent Ti 3 C 2 MXene quantum dots for macrophage labeling and Cu 2+ ion sensing. Nanoscale 11, 14123–14133. https://doi.org/10.1039/C9NR04421C.

Gund, G.S., Park, J.H., Harpalsinh, R., Kota, M., Shin, J.H., Kim, T. il, Gogotsi, Y., Park, H.S., 2019. MXene/polymer hybrid materials for flexible AC-filtering electrochemical capacitors. Joule 3, 164–176. https://doi.org/10.1016/j.joule.2018.10.017.

Hashtroudi, H., Mackinnon, I.D.R., Shafiei, M., 2020. Emerging 2D hybrid nanomaterials: towards enhanced sensitive and selective conductometric gas sensors at room temperature. J. Mater. Chem. C 8, 13108–13126. https://doi.org/10.1039/D0TC01968B.

He, J., Wu, P., Chen, L., Li, Hongping, Hua, M., Lu, L., Wei, Y., Chao, Y., Zhou, S., Zhu, W., Li, Huaming, 2021. Dynamically-generated TiO2 active site on MXene Ti3C2: boosting reactive desulfurization. Chem. Eng. J. 416, 129022 https://doi.org/10.1016/j.cej.2021.129022.

Ho, D.H., Choi, Y.Y., Jo, S.B., Myoung, J., Cho, J.H., 2021. Sensing with MXenes: progress and prospects. Adv. Mater. 33, 2005846 https://doi.org/10.1002/adma.202005846.

Huang, W., Hu, L., Tang, Y., Xie, Z., Zhang, H., 2020. Recent advances in functional 2D MXene-based nanostructures for next-generation devices. Adv. Funct. Mater. 30, 2005223 https://doi.org/10.1002/adfm.202005223.

Iqbal, A., Hong, J., Ko, T.Y., Koo, C.M., 2021. Improving oxidation stability of 2D MXenes: synthesis, storage media, and conditions. Nano Converg 8, 9. https://doi.org/10.1186/s40580-021-00259-6.

Jiang, G., Yang, R., Liu, J., Liu, H., Liu, L., Wu, Y.A.Y., 2022. Two-dimensional Ti2C MXene-induced photocurrent polarity switching photoelectrochemical biosensing platform for ultrasensitive and selective detection of soluble CD146. Sens. Actuators, B 350, 130859. https://doi.org/10.1016/j.snb.2021.130859.

Jiang, X., Kuklin, A.V., Baev, A., Ge, Y., Ågren, H., Zhang, H., Prasad, P.N., 2020. Two-dimensional MXenes: from morphological to optical, electric, and magnetic properties and applications. Phys. Rep. 848, 1–58. https://doi.org/10.1016/j.physrep.2019.12.006.

Jin, X., Liu, C., Xu, T., Su, L., Zhang, X., 2020. Artificial intelligence biosensors: challenges and prospects. Biosens. Bioelectron. 165, 112412 https://doi.org/10.1016/j.bios.2020.112412.

Kaushik, A., Jayant, R.D., Nair, M., 2018. Nanomedicine for neuroHIV/AIDS management. Nanomedicine 13, 669–673. https://doi.org/10.2217/nnm-2018-0005.

Kaushik, A., Kumar, R., Arya, S.K., Nair, M., Malhotra, B.D., Bhansali, S., 2015. Organic–inorganic hybrid nanocomposite-based gas sensors for environmental monitoring. Chem. Rev. 115, 4571–4606. https://doi.org/10.1021/cr400659h.

Kaushik, A.K., Dhau, J.S., Gohel, H., Mishra, Y.K., Kateb, B., Kim, N.-Y., Goswami, D.Y., 2020. Electrochemical SARS-CoV-2 sensing at point-of-care and artificial intelligence for intelligent COVID-19 management. ACS Appl. Bio Mater. 3, 7306–7325. https://doi.org/10.1021/acsabm.0c01004.

Khalediali dusti, R., Mishra, A.K., Barnoush, A., 2020. Atomic defects in monolayer ordered double transition metal carbide (Mo 2 TiC 2 T x) MXene and CO 2 adsorption. J. Mater. Chem. C 8, 4771–4779. https://doi.org/10.1039/C9TC06046D.

Khazaei, M., Arai, M., Sasaki, T., Chung, C.-Y., Venkataramanan, N.S., Estili, M., Sakka, Y., Kawazoe, Y., 2013. Novel electronic and magnetic properties of two-dimensional transition metal carbides and nitrides. Adv. Funct. Mater. 23, 2185–2192. https://doi.org/10.1002/adfm.201202502.

Khunger, A., Kaur, N., Mishra, Y.K., Ram Chaudhary, G., Kaushik, A., 2021. Perspective and prospects of 2D MXenes for smart biosensing. Mater. Lett. 304, 130656 https://doi.org/10.1016/j.matlet.2021.130656.

Kim, D.W., Lee, J.H., Kim, J.K., Jeong, U., 2020. Material aspects of triboelectric energy generation and sensors. NPG Asia Mater. 12, 6. https://doi.org/10.1038/s41427-019-0176-0.

Kim, J., Campbell, A.S., de Ávila, B.E.-F., Wang, J., 2019. Wearable biosensors for healthcare monitoring. Nat. Biotechnol. 37, 389–406. https://doi.org/10.1038/s41587-019-0045-y.

Kim, J., Imani, S., de Araujo, W.R., Warchall, J., Valdés-Ramírez, G., Paixão, T.R.L.C., Mercier, P.P., Wang, J., 2015. Wearable salivary uric acid mouthguard biosensor with integrated wireless electronics. Biosens. Bioelectron. 74, 1061–1068. https://doi.org/10.1016/j.bios.2015.07.039.

Kukhtin, A.C., Sebastian, T., Golova, J., Perov, A., Knickerbocker, C., Linger, Y., Bueno, A., Qu, P., Villanueva, M., Holmberg, R.C., Chandler, D.P., Cooney, C.G., 2019. Lab-on-a-Film disposable for genotyping multidrug-resistant Mycobacterium tuberculosis from sputum extracts. Lab Chip 19, 1217–1225. https://doi.org/10.1039/C8LC01404C.

Lashgari, H., Abolhassani, M.R., Boochani, A., Elahi, S.M., Khodadadi, J., 2014. Electronic and optical properties of 2D graphene-like compounds titanium carbides and nitrides: DFT calculations. Solid State Commun. 195, 61–69. https://doi.org/10.1016/j.ssc.2014.06.008.

Lee, Y., Kim, S.J., Kim, Y.-J., Lim, Y., Chae, Y., Lee, B.-J., Kim, Y.-T., Han, H., Gogotsi, Y., Ahn, C.W., 2020. Oxidation-resistant titanium carbide MXene films. J. Mater. Chem. 8, 573–581. https://doi.org/10.1039/C9TA07036B.

Lei, D., Liu, N., Su, T., Wang, L., Su, J., Zhang, Z., Gao, Y., 2020. Research progress of MXenes-based wearable pressure sensors. Apl. Mater. 8, 110702 https://doi.org/10.1063/5.0026984.

Lei, Y., Zhao, W., Zhang, Y., Jiang, Q., He, J., Baeumner, A.J., Wolfbeis, O.S., Wang, Z.L., Salama, K.N., Alshareef, H.N., 2019. A MXene-based wearable biosensor system for high-performance in vitro perspiration analysis. Small 15, 1901190. https://doi.org/10.1002/smll.201901190.

Li, H., Wen, Y., Zhu, X., Wang, J., Zhang, L., Sun, B., 2020. Novel heterostructure of a MXene@NiFe-LDH nanohybrid with superior peroxidase-like activity for sensitive colorimetric detection of glutathione. ACS Sustain. Chem. Eng. 8, 520–526. https://doi.org/10.1021/acssuschemeng.9b05987.

Li, M., Fang, L., Zhou, H., Wu, F., Lu, Y., Luo, H., Zhang, Y., Hu, B., 2019. Three-dimensional porous MXene/NiCo-LDH composite for high performance non-enzymatic glucose sensor. Appl. Surf. Sci. 495, 143554 https://doi.org/10.1016/j.apsusc.2019.143554.

Li, Q., Li, X., Zhou, P., Chen, R., Xiao, R., Pang, Y., 2022. Split aptamer regulated CRISPR/Cas12a biosensor for 17β-estradiol through a gap-enhanced Raman tags based lateral flow strategy. Biosens. Bioelectron. 215, 114548 https://doi.org/10.1016/j.bios.2022.114548.

Li, Q., Li, Y., Zeng, W., 2021. Preparation and application of 2D MXene-based gas sensors: a review. Chemosensors 9, 225. https://doi.org/10.3390/chemosensors9080225.

Li, S., Zhang, Yong, Wang, Y., Xia, K., Yin, Z., Wang, Huimin, Zhang, M., Liang, X., Lu, H., Zhu, M., Wang, Haomin, Shen, X., Zhang, Yingying, 2020. Physical sensors for skin-inspired electronics. InfoMat 2, 184–211. https://doi.org/10.1002/inf2.12060.

Li, X., Xu, J., Jiang, Y., He, Z., Liu, B., Xie, H., Li, H., Li, Z., Wang, Y., Tai, H., 2020. Toward agricultural ammonia volatilization monitoring: a flexible polyaniline/Ti3C2T hybrid sensitive films based gas sensor. Sens. Actuators, B 316, 128144. https://doi.org/10.1016/j.snb.2020.128144.

Li, Y., Kang, Z., Kong, L., Shi, H., Zhang, Y., Cui, M., Yang, D.-P., 2019. MXene-Ti3C2/CuS nanocomposites: enhanced peroxidase-like activity and sensitive colorimetric cholesterol detection. Mater. Sci. Eng. C 104, 110000. https://doi.org/10.1016/j.msec.2019.110000.

Li, Y., Peng, Z., Holl, N.J., Hassan, M.R., Pappas, J.M., Wei, C., Izadi, O.H., Wang, Y., Dong, X., Wang, C., Huang, Y.-W., Kim, D., Wu, C., 2021. MXene–graphene field-effect transistor sensing of influenza virus and SARS-CoV-2. ACS Omega 6, 6643–6653. https://doi.org/10.1021/acsomega.0c05421.

Lin, S., Lin, H., Yang, M., Ge, M., Chen, Y., Zhu, Y., 2020. A two-dimensional MXene potentiates a therapeutic microneedle patch for photonic implantable medicine in the second NIR biowindow. Nanoscale 12, 10265–10276. https://doi.org/10.1039/D0NR01444C.

Lipatov, A., Lu, H., Alhabeb, M., Anasori, B., Gruverman, A., Gogotsi, Y., Sinitskii, A., 2018. Elastic properties of 2D Ti 3 C 2 T x MXene monolayers and bilayers. Sci. Adv. 4 https://doi.org/10.1126/sciadv.aat0491.

Lipton, J., Röhr, J.A., Dang, V., Goad, A., Maleski, K., Lavini, F., Han, M., Tsai, E.H.R., Weng, G.-M., Kong, J., Riedo, E., Gogotsi, Y., Taylor, A.D., 2020. Scalable, highly conductive, and micropatternable MXene films for enhanced electromagnetic interference shielding. Matter 3, 546–557. https://doi.org/10.1016/j.matt.2020.05.023.

Liu, J., Jiang, X., Zhang, R., Zhang, Y., Wu, L., Lu, W., Li, J., Li, Y., Zhang, H., 2019. MXene-Enabled electrochemical microfluidic biosensor: applications toward multicomponent continuous monitoring in whole blood. Adv. Funct. Mater. 29, 1807326 https://doi.org/10.1002/adfm.201807326.

Liu, M., He, Y., Zhou, J., Ge, Y., Zhou, J., Song, G., 2020. A ''naked-eye'' colorimetric and ratiometric fluorescence probe for uric acid based on Ti3C2 MXene quantum dots. Anal. Chim. Acta 1103, 134–142. https://doi.org/10.1016/j.aca.2019.12.069.

Liu, M., Zhou, J., He, Y., Cai, Z., Ge, Y., Zhou, J., Song, G., 2019. ε-Poly-L-lysine-protected Ti3C2 MXene quantum dots with high quantum yield for fluorometric determination of cytochrome c and trypsin. Microchim. Acta 186, 770. https://doi.org/10.1007/s00604-019-3945-0.

Liu, S.-J., Ma, K., Liu, L.-S., Wang, K., Zhang, Y.-A., Bi, Z.-R., Chen, Y.-X., Chen, K.-Z., Wang, C.-X., Qiao, S.-L., 2022. Point-of-care non-invasive enzyme-cleavable nanosensors for acute transplant rejection detection. Biosens. Bioelectron. 215, 114568 https://doi.org/10.1016/j.bios.2022.114568.

Liu, X., Qiu, Y., Jiang, D., Li, F., Gan, Y., Zhu, Y., Pan, Y., Wan, H., Wang, P., 2022. Covalently grafting first-generation PAMAM dendrimers onto MXenes with self-adsorbed AuNPs for use as a functional nanoplatform for highly sensitive electrochemical biosensing of cTnT. Microsyst. Nanoeng. 8, 35. https://doi.org/10.1038/s41378-022-00352-8.

Mani, V., Chikkaveeraiah, B.V., Patel, V., Gutkind, J.S., Rusling, J.F., 2009. Ultrasensitive immunosensor for cancer biomarker proteins using gold nanoparticle film electrodes and multienzyme-particle amplification. ACS Nano 3, 585–594. https://doi.org/10.1021/nn800863w.

Mannoor, M.S., Tao, H., Clayton, J.D., Sengupta, A., Kaplan, D.L., Naik, R.R., Verma, N., Omenetto, F.G., McAlpine, M.C., 2012. Graphene-based wireless bacteria detection on tooth enamel. Nat. Commun. 3, 763. https://doi.org/10.1038/ncomms1767.

Markandan, K., Tiong, Y.W., Sankaran, R., Subramanian, S., Markandan, U.D., Chaudhary, V., Numan, A., Khalid, M., Walvekar, R., 2022. Emergence of infectious diseases and role of advanced nanomaterials in point-of-care diagnostics: a review. Biotechnology and Genetic Engineering Reviews. https://doi.org/10.1080/02648725.2022.2127070.

Mi, X., Li, H., Tan, R., Feng, B., Tu, Y., 2021. The TDs/aptamer cTnI biosensors based on HCR and Au/Ti3C2-MXene amplification for screening serious patient in COVID-19 pandemic. Biosens. Bioelectron. 192, 113482 https://doi.org/10.1016/j.bios.2021.113482.

Naguib, M., Barsoum, M.W., Gogotsi, Y., 2021. Ten years of progress in the synthesis and development of MXenes. Adv. Mater. 33, 2103393 https://doi.org/10.1002/adma.202103393.

Naguib, M., Kurtoglu, M., Presser, V., Lu, J., Niu, J., Heon, M., Hultman, L., Gogotsi, Y., Barsoum, M.W., 2011. Two-dimensional nanocrystals produced by exfoliation of Ti3AlC2. Adv. Mater. 23, 4248–4253. https://doi.org/10.1002/adma.201102306.

Natu, V., Hart, J.L., Sokol, M., Chiang, H., Taheri, M.L., Barsoum, M.W., 2019. Edge capping of 2D-MXene sheets with polyanionic salts to mitigate oxidation in aqueous colloidal suspensions. Angew. Chem. Int. Ed. 58, 12655–12660. https://doi.org/10.1002/anie.201906138.

Nayak, S., Patgiri, R., Member, S., 2020. 6G Communication Technology: A Vision on Intelligent Healthcare. IEEE Internet Things J.

Neampet, S., Ruecha, N., Qin, J., Wonsawat, W., Chailapakul, O., Rodthongkum, N., 2019. A nanocomposite prepared from platinum particles, polyaniline and a Ti3C2 MXene for amperometric sensing of hydrogen peroxide and lactate. Microchim. Acta 186, 752. https://doi.org/10.1007/s00604-019-3845-3.

Nguyen, D.C., Ding, M., Pathirana, P.N., Seneviratne, A., Li, J., Niyato, D., Dobre, O., Poor, H.V., 2022. 6G internet of things: a comprehensive survey. IEEE Internet Things J. 9 https://doi.org/10.1109/JIOT.2021.3103320.

Noh, S., Lee, H., Kim, J., Jang, H., An, J., Park, C., Lee, M.-H., Lee, T., 2022. Rapid electrochemical dual-target biosensor composed of an Aptamer/MXene hybrid on Au microgap electrodes for cytokines detection. Biosens. Bioelectron. 207, 114159 https://doi.org/10.1016/j.bios.2022.114159.

Novoselov, K.S., Geim, A.K., Morozov, S.V., Jiang, D., Zhang, Y., Dubonos, S.V., Grigorieva, I.V., Firsov, A.A., 2004. Electric field effect in atomically thin carbon films. Science (80-.) 306, 666–669. https://doi.org/10.1126/science.1102896.

Pan, H., Dong, Y., Gong, L., Zhai, J., Song, C., Ge, Z., Su, Y., Zhu, D., Chao, J., Su, S., Wang, L., Wan, Y., Fan, C., 2022. Sensing gastric cancer exosomes with MoS2-based SERS aptasensor. Biosens. Bioelectron. 215, 114553 https://doi.org/10.1016/j.bios.2022.114553.

Patel, S., Nanda, R., Sahoo, S., Mohapatra, E., 2016. Biosensors in health care: the milestones achieved in their development towards lab-on-chip-analysis. Biochem. Res. Int. 1–12 https://doi.org/10.1155/2016/3130469, 2016.

Pathania, D., Kumar, S., Thakur, P., Chaudhary, V., Kaushik, A., Varma, R.S., Furukawa, H., Sharma, M., Khosla, A., 2022. Essential oil-mediated biocompatible magnesium nanoparticles with enhanced antibacterial, antifungal, and photocatalytic efficacies. Sci. Rep. 12, 11431 https://doi.org/10.1038/s41598-022-14984-3.

Qian, S., Cui, Y., Cai, Z., Li, L., 2022. Applications of smartphone-based colorimetric biosensors. Biosens. Bioelectron. X 11, 100173. https://doi.org/10.1016/j.biosx.2022.100173.

Qiu, Z., Fan, D., Xue, X., Guo, S., Lin, Y., Chen, Y., Tang, D., 2022. Molecularly imprinted polymer functionalized Bi2S3/Ti3C2TX MXene nanocomposites for photoelectrochemical/electrochemical dual-mode sensing of chlorogenic acid. Chemosensors 10, 252. https://doi.org/10.3390/chemosensors10070252.

Rasheed, P.A., Pandey, R.P., Jabbar, K.A., Ponraj, J., Mahmoud, K.A., 2019. Sensitive electrochemical detection of <scp>l</scp> -cysteine based on a highly stable Pd@ Ti $_3$ C $_2$ T $_x$ (MXene) nanocomposite modified glassy carbon electrode. Anal. Methods 11, 3851–3856. https://doi.org/10.1039/C9AY00912D.

Scheller, F.W., Schubert, F., Neumann, B., Pfeiffer, D., Hintsche, R., Dransfeld, I., Wollenberger, U., Renneberg, R., Warsinke, A., Johansson, G., Skoog, M., Yang, X., Bogdanovskaya, V., Bückmann, A., Zaitsev, S.Y., 1991. Second generation biosensors. Biosens. Bioelectron. 6, 245–253. https://doi.org/10.1016/0956-5663(91)80010-U.

Scott, A., Pandey, R., Saxena, S., Osman, E., Li, Y., Soleymani, L., 2022. A smartphone operated electrochemical reader and actuator that streamlines the operation of electrochemical biosensors. ECS Sensors Plus 1, 014601. https://doi.org/10.1149/2754-2726/AC5FB3.

Seitz, W.R., 1984. Chemical sensors based on fiber optics. Anal. Chem. 56, 16A–34A. https://doi.org/10.1021/ac00265a711.

Shahzad, F., Iqbal, A., Zaidi, S.A., Hwang, S.-W., Koo, C.M., 2019. Nafion-stabilized two-dimensional transition metal carbide (Ti3C2Tx MXene) as a high-performance electrochemical sensor for neurotransmitter. J. Ind. Eng. Chem. 79, 338–344. https://doi.org/10.1016/j.jiec.2019.03.061.

Sheth, Y., Dharaskar, S., Chaudhary, V., Khalid, M., Walvekar, R., 2022. Prospects of titanium carbide-based MXene in heavy metal ion and radionuclide adsorption for wastewater remediation: a review. Chemosphere 293, 133563. https://doi.org/10.1016/j.chemosphere.2022.133563.

Shuck, C.E., Sarycheva, A., Anayee, M., Levitt, A., Zhu, Y., Uzun, S., Balitskiy, V., Zahorodna, V., Gogotsi, O., Gogotsi, Y., 2020. Scalable synthesis of Ti 3 C 2 T x MXene. Adv. Eng. Mater. 22, 1901241 https://doi.org/10.1002/adem.201901241.

Si, C., Jin, K.-H., Zhou, J., Sun, Z., Liu, F., 2016. Large-gap quantum spin Hall state in MXenes: d -band topological order in a triangular lattice. Nano Lett. 16, 6584–6591. https://doi.org/10.1021/acs.nanolett.6b03118.

Singh, K.R., Nayak, V., Singh, J., Singh, R.P., 2021. Nano-enabled wearable sensors for the internet of things (IoT). Mater. Lett. 304, 130614 https://doi.org/10.1016/j.matlet.2021.130614.

Solanki, P.R., Kaushik, A., Agrawal, V.V., Malhotra, B.D., 2011. Nanostructured metal oxide-based biosensors. NPG Asia Mater. 3, 17–24. https://doi.org/10.1038/asiamat.2010.137.

Sonu, Chaudhary, V., 2022. A Paradigm of Internet-of-Nano-Things Inspired Intelligent Plant Pathogen-Diagnostic Biosensors. ECS Sensor Plus 1 (031401). https://doi.org/10.1149/2754-2726/ac92ed.

Tan, P., Zou, Y., Fan, Y., Li, Z., 2020. Self-powered wearable electronics. Wearable Technol. 1, e5. https://doi.org/10.1017/wtc.2020.3.

Tiwari, S., Atluri, V., Kaushik, A., Yndart, A., Nair, M., 2019. Alzheimer's disease: pathogenesis, diagnostics, and therapeutics. Int. J. Nanomed. 14, 5541–5554. https://doi.org/10.2147/IJN.S200490.

Unal, M.A., Bayrakdar, F., Fusco, L., Besbinar, O., Shuck, C.E., Yalcin, S., Erken, M.T., Ozkul, A., Gurcan, C., Panatli, O., Summak, G.Y., Gokce, C., Orecchioni, M., Gazzi, A., Vitale, F., Somers, J., Demir, E., Yildiz, S.S., Nazir, H., Grivel, J.-C., Bedognetti, D., Crisanti, A., Akcali, K.C., Gogotsi, Y., Delogu, L.G., Yilmazer, A., 2021. 2D MXenes with antiviral and immunomodulatory properties: a pilot study against SARS-CoV-2. Nano Today 38, 101136. https://doi.org/10.1016/j.nantod.2021.101136.

Verma, D., Singh, K.R., Yadav, A.K., Nayak, V., Singh, J., Solanki, P.R., Singh, R.P., 2022. Internet of things (IoT) in nano-integrated wearable biosensor devices for healthcare applications. Biosens. Bioelectron. X 11, 100153. https://doi.org/10.1016/j.biosx.2022.100153.

Verma, N., Bhardwaj, A., 2015. Biosensor technology for pesticides—a review. Appl. Biochem. Biotechnol. 175, 3093–3119. https://doi.org/10.1007/s12010-015-1489-2.

Wan, S., Li, X., Chen, Y., Liu, N., Du, Y., Dou, S., Jiang, L., Cheng, Q., 2021. High-strength scalable MXene films through bridging-induced densification. Science 80–, 96–99. https://doi.org/10.1126/science.abg2026, 374.

Wang, H., Li, H., Huang, Y., Xiong, M., Wang, F., Li, C., 2019. A label-free electrochemical biosensor for highly sensitive detection of gliotoxin based on DNA nanostructure/MXene nanocomplexes. Biosens. Bioelectron. 142, 111531 https://doi.org/10.1016/j.bios.2019.111531.

Wang, L., Zhang, H., Zhuang, T., Liu, J., Sojic, N., Wang, Z., 2022. Sensitive electrochemiluminescence biosensing of polynucleotide kinase using the versatility of two-dimensional Ti3C2TX MXene nanomaterials. Anal. Chim. Acta 1191, 339346. https://doi.org/10.1016/j.aca.2021.339346.

Wang, L., Zhang, M., Yang, B., Tan, J., Ding, X., Li, W., 2021. Recent advances in multidimensional (1D, 2D, and 3D) composite sensors derived from MXene: synthesis, structure, application, and perspective. Small Methods 5, 2100409. https://doi.org/10.1002/smtd.202100409.

Wang, S., Jiang, Y., Liu, B., Duan, Z., Pan, H., Yuan, Z., Xie, G., Wang, J., Fang, Z., Tai, H., 2021a. Ultrathin Nb2CT nanosheets-supported polyaniline nanocomposite: enabling ultrasensitive NH3 detection. Sens. Actuators, B 343, 130069. https://doi.org/10.1016/j.snb.2021.130069.

Wang, S., Liu, B., Duan, Z., Zhao, Q., Zhang, Y., Xie, G., Jiang, Y., Li, S., Tai, H., 2021b. PANI nanofibers-supported Nb2CTx nanosheets-enabled selective NH3 detection driven by TENG at room temperature. Sens. Actuators, B 327, 128923. https://doi.org/10.1016/j.snb.2020.128923.

Wang, Y., Huo, T., Du, Y., Qian, M., Lin, C., Nie, H., Li, W., Hao, T., Zhang, X., Lin, N., Huang, R., 2022. Sensitive CTC analysis and dual-mode MRI/FL diagnosis based on a magnetic core-shell aptasensor. Biosens. Bioelectron. 215, 114530 https://doi.org/10.1016/j.bios.2022.114530.

Wei, Y., Zhang, P., Soomro, R.A., Zhu, Q., Xu, B., 2021. Advances in the synthesis of 2D MXenes. Adv. Mater. 33, 2103148 https://doi.org/10.1002/adma.202103148.

Weng, H., Ranjbar, A., Liang, Y., Song, Z., Khazaei, M., Yunoki, S., Arai, M., Kawazoe, Y., Fang, Z., Dai, X., 2015. Large-gap two-dimensional topological insulator in oxygen functionalized MXene. Phys. Rev. B 92, 075436. https://doi.org/10.1103/PhysRevB.92.075436.

Wu, C., Zhang, X., Wang, R., Chen, L.J., Nie, M., Zhang, Z., Huang, X., Han, L., 2022. Low-dimensional material based wearable sensors. Nanotechnology 33, 072001. https://doi.org/10.1088/1361-6528/ac33d1.

Wu, D., Wu, M., Yang, J., Zhang, H., Xie, K., Lin, C.-T., Yu, A., Yu, J., Fu, L., 2019. Delaminated Ti3C2Tx (MXene) for electrochemical carbendazim sensing. Mater. Lett. 236, 412–415. https://doi.org/10.1016/j.matlet.2018.10.150.

Wu, X., Wang, Z., Yu, M., Xiu, L., Qiu, J., 2017. Stabilizing the MXenes by carbon nanoplating for developing hierarchical nanohybrids with efficient lithium storage and hydrogen evolution capability. Adv. Mater. 29, 1607017 https://doi.org/10.1002/adma.201607017.

Xi, X., Wang, J., Wang, Y., Xiong, H., Chen, M., Wu, Z., Zhang, X., Wang, S., Wen, W., 2022. Preparation of Au/Pt/Ti3C2Cl2 nanoflakes with self-reducing method for colorimetric detection of glutathione and intracellular sensing of hydrogen peroxide. Carbon N. Y. https://doi.org/10.1016/j.carbon.2022.06.068.

Xie, Y., Kent, P.R.C., 2013. Hybrid density functional study of structural and electronic properties of functionalized \ce{Ti_{n+1}X_n} (X= C, N) monolayers. Phys. Rev. B 87, 235441. https://doi.org/10.1103/PhysRevB.87.235441.

Xin, M., Li, J., Ma, Z., Pan, L., Shi, Y., 2020. MXenes and their applications in wearable sensors. Front. Chem. 8 https://doi.org/10.3389/fchem.2020.00297.

Xue, Q., Zhang, H., Zhu, M., Pei, Z., Li, H., Wang, Z., Huang, Yang, Huang, Yan, Deng, Q., Zhou, J., Du, S., Huang, Q., Zhi, C., 2017. Photoluminescent Ti 3 C 2 MXene quantum dots for multicolor cellular imaging. Adv. Mater. 29, 1604847 https://doi.org/10.1002/adma.201604847.

Xun, G., Lane, S.T., Petrov, V.A., Pepa, B.E., Zhao, H., 2021. A rapid, accurate, scalable, and portable testing system for COVID-19 diagnosis. Nat. Commun. 12, 2905. https://doi.org/10.1038/s41467-021-23185-x.

Yang, Y.-C., Lin, Y.-T., Yu, J., Chang, H.-T., Lu, T.-Y., Huang, T.-Y., Preet, A., Hsu, Y.-J., Wang, L., Lin, T.-E., 2021. MXene nanosheet-based microneedles for monitoring muscle contraction and electrostimulation treatment. ACS Appl. Nano Mater. 4, 7917–7924. https://doi.org/10.1021/acsanm.1c01237.

Yao, B., Zhang, J., Fan, Z., Ding, Y., Zhou, B., Yang, R., Zhao, J., Zhang, K., 2021. Rational engineering of the DNA walker amplification strategy by using a Au@Ti 3 C 2 @PEI-Ru(dcbpy) 3 2+ nanocomposite biosensor for detection of the SARS-CoV-2 RdRp gene. ACS Appl. Mater. Interfaces 13, 19816–19824. https://doi.org/10.1021/acsami.1c04453.

Yao, Y., Lan, L., Liu, X., Ying, Y., Ping, J., 2020. Spontaneous growth and regulation of noble metal nanoparticles on flexible biomimetic MXene paper for bioelectronics. Biosens. Bioelectron. 148, 111799 https://doi.org/10.1016/j.bios.2019.111799.

Zha, X.-H., Zhou, J., Eklund, P., Bai, X., Du, S., Huang, Q., 2019. Non-MAX phase precursors for MXenes. In: 2D Metal Carbides and Nitrides (MXenes). Springer International Publishing, Cham, pp. 53–68. https://doi.org/10.1007/978-3-030-19026-2_4.

Zhan, X., Si, C., Zhou, J., Sun, Z., 2020. MXene and MXene-based composites: synthesis, properties and environment-related applications. Nanoscale Horizons 5, 235–258. https://doi.org/10.1039/C9NH00571D.

Zhang, C.J., Pinilla, S., McEvoy, N., Cullen, C.P., Anasori, B., Long, E., Park, S.-H., Seral-Ascaso, A., Shmeliov, A., Krishnan, D., Morant, C., Liu, X., Duesberg, G.S., Gogotsi, Y., Nicolosi, V., 2017. Oxidation stability of colloidal two-dimensional titanium carbides (MXenes). Chem. Mater. 29, 4848–4856. https://doi.org/10.1021/acs.chemmater.7b00745.

Zhang, H., He, R., Niu, Y., Han, F., Li, J., Zhang, X., Xu, F., 2022. Graphene-enabled wearable sensors for healthcare monitoring. Biosens. Bioelectron. 197, 113777 https://doi.org/10.1016/j.bios.2021.113777.

Zhang, H., Wang, Z., Zhang, Q., Wang, F., Liu, Y., 2019. Ti3C2 MXenes nanosheets catalyzed highly efficient electrogenerated chemiluminescence biosensor for the detection of exosomes. Biosens. Bioelectron. 124–125, 184–190. https://doi.org/10.1016/j.bios.2018.10.016.

Zhang, J., Kong, N., Uzun, S., Levitt, A., Seyedin, S., Lynch, P.A., Qin, S., Han, M., Yang, W., Liu, J., Wang, X., Gogotsi, Y., Razal, J.M., 2020. Scalable manufacturing of free-standing, strong Ti 3 C 2 T x MXene films with outstanding conductivity. Adv. Mater. 32, 2001093 https://doi.org/10.1002/adma.202001093.

Zhang, K., Fan, Z., Huang, Y., Ding, Y., Xie, M., 2022. A strategy combining 3D-DNA Walker and CRISPR-Cas12a trans-cleavage activity applied to MXene based electrochemiluminescent sensor for SARS-CoV-2 RdRp gene detection. Talanta 236, 122868. https://doi.org/10.1016/j.talanta.2021.122868.

Zhang, S., Huang, P., Wang, J., Zhuang, Z., Zhang, Z., Han, W.-Q., 2020. Fast and universal solution-phase flocculation strategy for scalable synthesis of various few-layered MXene powders. J. Phys. Chem. Lett. 11, 1247–1254. https://doi.org/10.1021/acs.jpclett.9b03682.

Zhang, W., Li, G., 2004. Third-generation biosensors based on the direct electron transfer of proteins. Anal. Sci. 20, 603–609. https://doi.org/10.2116/analsci.20.603.

Zhang, W., Pan, Z., Ma, J., Wei, L., Chen, Z., Wang, J., 2022. Degradable cross-linked collagen fiber/MXene composite aerogels as a high-performing sensitive pressure

sensor. ACS Sustain. Chem. Eng. 10, 1408–1418. https://doi.org/10.1021/acssuschemeng.1c05757.

Zhang, Y., Jiang, X., Zhang, J., Zhang, H., Li, Y., 2019. Simultaneous voltammetric determination of acetaminophen and isoniazid using MXene modified screen-printed electrode. Biosens. Bioelectron. 130, 315–321. https://doi.org/10.1016/j.bios.2019.01.043.

Zhao, J., He, C., Wu, W., Yang, H., Dong, J., Wen, L., Hu, Z., Yang, M., Hou, C., Huo, D., 2022. MXene-MoS2 heterostructure collaborated with catalyzed hairpin assembly for label-free electrochemical detection of microRNA-21. Talanta 237, 122927. https://doi.org/10.1016/j.talanta.2021.122927.

Zhao, L., Wang, K., Wei, W., Wang, L., Han, W., 2019. High-performance flexible sensing devices based on polyaniline/MXene nanocomposites. InfoMat 1, 407–416. https://doi.org/10.1002/inf2.12032.

Zhao, M.Q., Trainor, N., Ren, C.E., Torelli, M., Anasori, B., Gogotsi, Y., 2019. Scalable manufacturing of large and flexible sheets of MXene/graphene heterostructures. Adv. Mater. Technol. 4, 1800639 https://doi.org/10.1002/admt.201800639.

Zhao, X., Vashisth, A., Prehn, E., Sun, W., Shah, S.A., Habib, T., Chen, Y., Tan, Z., Lutkenhaus, J.L., Radovic, M., Green, M.J., 2019. Antioxidants unlock shelf-stable Ti3C2T (MXene) nanosheet dispersions. Matter 1, 513–526. https://doi.org/10.1016/j.matt.2019.05.020.

Zhou, T., Zhang, T., 2021. Recent progress of nanostructured sensing materials from 0D to 3D: overview of structure–property-application relationship for gas sensors. Small Methods 5, 2100515. https://doi.org/10.1002/smtd.202100515.